Supplementary Data

Following an Environmental Carcinogen N^2-dG Adduct through Replication: Elucidating Blockage and Bypass in a High-fidelity DNA Polymerase

Pingna Xu[†], *Lida Oum*[‡], *Lorena S. Beese*[£], *Nicholas E. Geacintov*[‡], *Suse Broyde*[†§]

[†]Department of Biology, New York University, New York, NY

[‡]Department of Chemistry, New York University, New York, NY

[£]Department of Biochemistry, Duke University Medical Center, Durham, NC

[§]To whom correspondence should be addressed: Suse Broyde: tel. (212)998-8231, fax (212)995-4015, e-mail broyde@nyu.edu

Running Title: Carcinogen Blockage and Bypass in DNA Replication.

Key Words: carcinogen; [BP]G* adduct; BF DNA polymerase; translesion synthesis; molecular dynamics simulation

Abbreviations: PAH, polycyclic aromatic hydrocarbon; BP, benzo[*a*]pyrene; BPDE, 7,8-dihydroxy-9,10-epoxybenzo[a]pyrene diol epoxide; (+)-*anti*-BPDE, (+)-7(R),8(S),9(S),10(R) BPDE; [BP]G*, (+)-*trans*-*anti*-[BP]-N^2-deoxyguanosine; dNTP, 2'-deoxynucleotide triphosphate; BF, bacillus fragment; CG, conjugate gradient; SD, steepest descent; MD, molecular dynamics; ps, picosecond; ns, nanosecond; RMSD, root mean square deviation; AF, aminofluorene; [AF]G*, *N*-(2'-deoxyguanosin-8-yl)-aminofluorene.

Molecular Modeling

Ternary Complex. One SO_4^{2-} group with no biological significance was deleted from the original crystal structure of the ternary complex. Hydrogen atoms missing from the crystal structure were added by the LEaP module in AMBER [1]. A hydroxyl group was added to the 3'-end of the primer since in the crystal structure, a dideoxynucleotide was used to prevent further incorporation of the incoming dNTP. We then remodeled the active site. The single BF crystal structure contained one catalytic Mg^{2+} ion and one Mn^{2+} ion presumably in the position of the nucleotide binding Mg^{2+} ion. We substituted this Mn^{2+} ion with a more biologically relevant Mg^{2+} ion. Then the positions of the two Mg^{2+} ions were slightly adjusted and one water molecule was added to achieve proper octahedral coordination. The catalytic Mg^{2+} ion chelates Oδ2 of ASP653, Oδ1 of ASP830, Oε2 of Glu831, O3' of the primer end, O2α of dNTP, and the oxygen atom of the added water molecule. The nucleotide binding Mg^{2+} ion chelates Oδ1 of ASP653, O of Tyr654, Oδ2 of ASP830, O2α, O2β and O2γ of dNTP. Figure S1 shows the octahedral coordination of the two Mg^{2+} ions.

Binary Complex. Five SO_4^{2-} groups and two sucrose molecules with no biological significance were deleted from the original crystal structure of the binary complex. There was one Mg^{2+} ion in the structure but not close to the 3'-O of the primer end. Since binary complexes do not appear to contain Mg^{2+} ions [2-4], we deleted it. Missing hydrogen atoms were added using LEaP.

Force Field Parameterization. New force field parameters need to be assigned to the modified residues for MD simulations if not present in the AMBER force field for standard protein and nucleic acid residues, or in GAFF [5]. The modified residues in this work included the [BP]G* adduct and the four incoming dNTPs.

We constructed both an *anti* (χ = 188.4°, α' = 124.7°, and β' = 232.9°) and a *syn* (χ = 15.7°, α' = 274.3°, and β' = 239.3°) BP modified deoxyguanosine structures and carried out quantum mechanical geometry optimization and electrostatic potential calculations for the two structures using Hartree-Fock method with basis set 6-31G* in GAUSSIAN 98 [6]. The least square charge-fitting algorithm, RESP was then employed to fit the charge to each atom [7]. Then, the charges were normalized so that [BP]G* has a charge of –1 [8]. The partial charges for the *anti*- and *syn*-[BP]G* are shown in Table S2. The conformation of [BP]G* (*anti* or *syn*) in a specific system determined which set of partial changes was used during MD. Partial charges for dATP, dGTP, dCTP and dTTP were computed previously [9]. Parameters added to the AMBER 7.0 force field for [BP]G* were assigned previously [9] by analogy to chemically similar atom types already available in the parm99 parameter set [10].

MD Simulation Protocol. MD simulations were carried out using the SANDER module of AMBER 7.0 [1] with the Cornell et al. force field [11] and the parm99.dat parameter set [10]. Long-range electrostatic interactions were approximated using the particle mesh Ewald method [12, 13], and a 9 Å cutoff was applied to the non-bonded Lennard-Jones interactions. The SHAKE algorithm [14] was employed to constrain all bonds involving hydrogen atoms with a tolerance of 10^{-6}, and a 2 fs time step was used in all dynamics simulations. Periodic boundary conditions were applied. The translational motion of the center of mass was removed at an interval of 1 ps.

The initial models were further prepared for MD by the LEaP module of AMBER 7.0. First, each system was neutralized with counterions. Thirty-three Na+ ions were added to each of the systems. Next, hydrogen atoms, Na+ ions and crystallographic water molecules were minimized by AMBER 7.0 for 600 steps of steepest descent (SD) followed by 400 steps of conjugate gradient (CG) while the solute (protein-DNA complex) was held fixed with harmonic restraints of 60 kcal/mol Å. Each system was then solvated with a rectangular box of TIP3P waters [15] extending 10 Å from the solute in each direction. To minimize the number of water molecules added to each system, the Simulaid program [16] was employed to optimize the orientation of the rectangular water box. About 25,000 water molecules were added to each system.

Then, Na+ ions and all the waters in each system were minimized by AMBER 7.0 for 100 steps of SD followed by 3900 steps of CG, while holding the solute fixed with harmonic restraints of 60 kcal/mol Å.

Each system was fully equilibrated prior to unrestrained MD. First, 30 ps MD was conducted at 10K with 20 kcal/mol Å restraints on the solute or part of the solute, while allowing the solvent to relax. In the systems with the [BP]G* in *syn* conformations, the protein-DNA complex was restrained. However, in the systems where [BP]G* is *anti*, only the DNA was restrained and the protein was relaxed. We had tried to restrain both protein and DNA during this step for *anti*-[BP]G*, but the subsequent equilibration failed due to a SHAKE problem stemming from more close contacts in these initial models. Next, each system was heated from 10K to 310K over 80 ps using the Berendsen coupling algorithm [17] with a coupling parameter of 0.5 ps, and then held at 310K for 20 ps with harmonic restraints of 20 kcal/mol Å on the solute. The rest of the equilibration was performed at 310K. The restraints on the solute were decreased slowly over 170 ps of MD by running 30 ps with 10 kcal/mol Å restraints, 40 ps with 1 kcal/mol Å restraints, 40 ps with 0.2 kcal/mol Å restraints and another 60 ps with 0 kcal/mol Å restraints. Finally, unrestrained production MD was started right after equilibration, at 310 K with a temperature coupling time constant of 4.0 ps and at atmospheric pressure with a 1.0 ps pressure relaxation time.

Table S1. Torsion angles (º) for [BP]G* in initial models at the four steps.

	χ	α'	β'
Step 1: [BP]G* at the Pre-insertion Site of Open BF			
anti-[BP]G*	211˚	276˚	215˚
syn-[BP]G*	51˚	43˚	235˚
Step 2: [BP]G* at the Insertion Site of Closed BF			
anti-[BP]G*	188˚	125˚	233˚
syn-[BP]G*	22˚	293˚	231˚
Step 3: [BP]G* at the Post-insertion Site of Open BF			
anti-1-[BP]G*	202˚	179˚	284˚
anti-2-[BP]G*	202˚	147˚	234˚
anti-3-[BP]G*	251˚	179˚	296˚
syn-[BP]G*	59˚	357˚	304˚
Step 4: [BP]G* at the Post-insertion Site of Closed BF			
anti-[BP]G*	211˚	102˚	234˚
syn-[BP]G*	56˚	232˚	243˚

Table S2. AMBER atom type, connection type, and partial charges of *anti*- and *syn*-[BP]G*.

Atom	AMBER atom type	Connection type	Partial charges of *anti*-[BP]G*	Partial charges of *syn*-[BP]G*
P	P	M	1.221635	1.220344
O1P	O2	E	-0.793760	-0.792451
O2P	O2	E	-0.793760	-0.792451
O5'	OS	M	-0.488727	-0.488880
C5'	CT	M	-0.023173	-0.001653
H5'1	H1	E	0.087625	0.079294
H5'2	H1	E	0.087625	0.079294
C4'	CT	M	0.091376	0.083341
H4'	H1	E	0.130786	0.109386
O4'	OS	S	-0.349694	-0.356587
C1'	CT	B	0.045171	0.131099
H1'	H2	E	0.159850	0.073468
N9	N*	B	0.012153	-0.068703
C4	CB	E	0.089340	0.005465
C8	CK	B	0.159083	0.128077
H8	H5	E	0.173852	0.162477
N7	NB	S	-0.595670	-0.560470
C5	CB	S	0.238408	0.281443
C6	C	B	0.478598	0.437102
O6	O	E	-0.539680	-0.539921
N1	NA	B	-0.430522	-0.262443
H1	H	E	0.323012	0.296194
C2	CA	B	0.515926	0.047887
N3	NC	E	-0.460478	-0.136580
N	N2	B	-0.642681	-0.352256
HN	H	E	0.378328	0.330451
CC10	CT	B	0.047029	-0.003702
HC10	H1	E	0.107661	0.095641
CC9	CT	3	-0.015315	0.022331
HC9	H1	E	0.120994	0.091023
O9	OH	S	-0.655097	-0.605140
H9	HO	E	0.443949	0.401289
CC8	CT	3	0.267880	0.220123
HC8	H1	E	0.105830	0.096197
O8	OH	S	-0.690495	-0.679699
HO8	HO	E	0.442214	0.436788
CC7	CT	3	0.154345	0.174907
HC7	H1	E	0.083532	0.040466
O7	OH	S	-0.667804	-0.648028
HO7	HO	E	0.439819	0.439166
C61	CA	S	-0.025802	-0.030552
CC6	CA	B	-0.163070	-0.156771
HC6	HA	E	0.172154	0.162272
C51	CA	B	0.012076	0.028555
C123	CA	E	0.024717	0.025805
CC5	CA	B	-0.164981	-0.167065
HC5	HA	E	0.143405	0.145191
CC4	CA	B	-0.194404	-0.185544
HC4	HA	E	0.147819	0.147599
C31	CA	B	0.040557	0.041082
C122	CA	E	0.122960	0.085822
CC3	CA	B	-0.153060	-0.136852
HC3	HA	E	0.144263	0.145333
CC2	CA	B	-0.203308	-0.217466
HC2	HA	E	0.159531	0.165953
CC1	CA	B	-0.154277	-0.138314
HC1	HA	E	0.147144	0.144636
C121	CA	S	0.039600	0.048444
CC12	CA	B	-0.210082	-0.204701
HC12	HA	E	0.157394	0.156943
CC11	CA	B	-0.168785	-0.154158
HC11	HA	E	0.154649	0.151745
C102	CA	S	-0.016382	-0.015237
C101	CA	E	0.018008	-0.039553
C3'	CT	M	0.044490	-0.024426
H3'	H1	E	0.124653	0.324895
C2'	CT	B	-0.054611	-0.042350
H2'1	HC	E	0.056044	0.043647
H2'2	HC	E	0.056044	0.043647
O3'	OS	M	-0.515911	-0.542870

Table S3: Michaelis – Menten parameters determined from steady-state catalytic efficiencies of dGTP and dATP incorporation opposite BP-modified guanine, G*. Pyrimidine dNTP insertion opposite G* is significantly lower under the experimental conditions of [DNA]/[BF] ratios used, and were not investigated further. Typical experimental results are shown in Figure S4.

DNA Polymerase	adduct sequence CG*G	base pairing	k_{cat} (min^{-1}) × 10^{-3}	K_m (μM)	f_{ins}($\mu M^{-1}min^{-1}$) (k_{cat}/K_m)
BF	CG*G	G*:dATP	56 ± 8.8	650 ± 180	8.7 x 10^{-5}
		G*:dGTP	17 ± 1.2	580 ± 130	3.0 x 10^{-5}
	CGG	G:dCTP	3900 ± 120	6.4 ± 0.98	0.60

Apparent k_{cat} values are calculated from $V_{max}/[E_0]$; $[E_0]$ is the total enzyme concentration. For adduct, [DNA]= 15 nM; [BF] = 2 nM; 37 ^{0}C. In the case of the unmodified sample, [DNA]= 20 nM; [BF] = 0.1 nM. The ratios f_{ins} (G)/f_{ins} (G*) are ~ 7,000 and 20,000 for dATP and dGTP insertion, respectively.

Table S4. Pre-insertion site width (Å)[a] in open BF (Step 1 and Step 3).

[BP]G* at the Pre-insertion Site of Open BF (Step 1)		
control	*anti*-[BP]G*	*syn*-[BP]G*
6.7±0.3	10.4±0.5 [b]	6.2±0.4

[BP]G* at the Post-insertion Site of Open BF (Step 3)							
control	*anti*-1-[BP]G*:dC	*anti*-2-[BP]G*:dC	*anti*-3-[BP]G*:dC	*Syn*-[BP]G*:dA	*syn*-[BP]G*:dC	*syn*-[BP]G*:dG	*syn*-[BP]G*:dT
6.3±0.3	6.6±0.3	6.1±0.3	6.6±0.3	6.8±0.3	6.7±0.4	6.5±0.3	7.1±0.6

[a] Ensemble average values and standard deviations are provided.

[b] Yellow highlighted number denotes a disruption.

Table S5. Hydrogen bond occupancies (%)[a] of base pairs involving [BP]G* and immediate neighbors.

[BP]G* at Pre-insertion Site of Open BF (Step 1)

Donor	Acceptor	control	*anti*-[BP]G*	*syn*-[BP]G*
G (T[a]) N2	C (P[b]) O2	99.7	99.2	98.9
G (T) N1	C (P) N3	99.8	100.0	99.5
C (P) N4	G (T) O6	96.7	97.5	92.6

[BP]G* at Insertion Site of Closed BF (Step 2)

Donor	Acceptor	control	*anti*-[BP]G*:dCTP	*syn*-[BP]G*:dATP	*syn*-[BP]G*:dCTP	*syn*-[BP]G*:dGTP	*syn*-[BP]G*:dTTP
[BP]G* (T) N2	dCTP O2	100	99.8	N/A	N/A	N/A	N/A
[BP]G* (T) N1	dCTP N3	99.9	85.5	N/A	N/A	N/A	N/A
dCTP N4	[BP]G* (T) O6	96.7	67.2[c]	N/A	N/A	N/A	N/A
dATP N6	[BP]G* (T) N7	N/A	N/A	73.3	N/A	N/A	N/A
dCTP N4	[BP]G* (T) O6	N/A	N/A	N/A	95.7	N/A	N/A
dGTP N2	[BP]G* (T) N7	N/A	N/A	N/A	N/A	99.2	N/A
dGTP N1	[BP]G* (T) O6	N/A	N/A	N/A	N/A	73.2	N/A
G (T) N2	C (P) O2	99.8	93.8	96.8	68.1	98.2	96.3
G (T) N1	C (P) N3	97.4	93.7	100.0	79.7	99.9	99.7
C (P) N4	G (T) O6	98.0	83.2	99.4	79.0	96.5	97.9

[BP]G* at Post-insertion Site of Open BF (Step 3)

Donor	Acceptor	control	*anti*-1-[BP]G*:dC	*anti*-2-[BP]G*:dC	*anti*-3-[BP]G*:dC	*syn*-[BP]G*:dA	*syn*-[BP]G*:dC	*syn*-[BP]G*:dG	*syn*-[BP]G*:dT
[BP]G* (T) N2	C (P) O2	99.8	100.0	100.0	100.0	N/A	N/A	N/A	N/A
[BP]G* (T) N1	C (P) N3	99.9	99.0	95.0	99.9	N/A	N/A	N/A	N/A
C (P) N4	[BP]G* (T) O6	96.3	86.9	86.7	99.2	N/A	N/A	N/A	N/A
A (P) N6	[BP]G* (T) N7	N/A	N/A	N/A	N/A	71.3	N/A	N/A	N/A
C (P) N4	[BP]G* (T) N7	N/A	N/A	N/A	N/A	N/A	24.4	N/A	N/A
G (P) N2	[BP]G* (T) N7	N/A	N/A	N/A	N/A	N/A	N/A	32.4	N/A
G (P) N1	[BP]G* (T) N7	N/A	N/A	N/A	N/A	N/A	N/A	76.5	N/A
G (T) N2	C (P) O2	98.6	93.2	96.0	99.9	99.8	99.0	99.0	97.7
G (T) N1	C (P) N3	99.9	99.5	96.0	99.4	100.0	99.7	99.9	99.7
C (P) N4	G (T) O6	98.7	99.4	91.3	93.6	98.0	98.2	98.6	99.7

[BP]G* at Post-insertion Site of Closed BF (Step 4)

Donor	Acceptor	control	*anti*-[BP]G*:dC	*syn*-[BP]G*:dA	*syn*-[BP]G*:dC	*syn*-[BP]G*:dG	*syn*-[BP]G*:dT
C (T) N4	dGTP O6	97.4	96.5	97.4	97.8	75.1	96.9
dGTP N2	C (T) O2	100.0	93.3	99.7	99.6	99.5	100.0
dGTP N1	C (T) N3	99.9	99.3	99.8	99.9	96.7	99.4
[BP]G* (T) N2	C (P) O2	99.2	1.6	N/A	N/A	N/A	N/A
[BP]G* (T) N1	C (P) N3	99.8	6.0	N/A	N/A	N/A	N/A
C (P) N4	[BP]G* (T) O6	99.3	52.0	N/A	N/A	N/A	N/A
A (P) N6	[BP]G* (T) N7	N/A	N/A	87.7	N/A	N/A	N/A
C (P) N4	[BP]G* (T) N7	N/A	N/A	N/A	73.8	N/A	N/A
G (P) N2	[BP]G* (T) N7	N/A	N/A	N/A	N/A	84.2	N/A
G (P) N1	[BP]G* (T) O6	N/A	N/A	N/A	N/A	99.9	N/A
T (P) N3	[BP]G* (T) N7	N/A	N/A	N/A	N/A	N/A	87.6
G (T) N2	C (P) O2	99.8	97.7	98.6	98.3	98.6	95.1
G (T) N1	C (P) N3	100.0	100.0	100.0	99.8	99.7	98.7
C (P) N4	G (T) O6	98.7	99.7	98.2	99.2	98.3	95.9

[a] % occupied indicates percentage of the time (time range, 0.8-2 ns) that the hydrogen bond was intact. Hydrogen bonding criteria were 3.3 Å between heavy atoms and a hydrogen bonding angle of 135º. Grey-shaded region, non-shaded region, and green-shaded region denote hydrogen bonds in the 0, +1 and +2 base pairs, respectively.

[b] T is the base on the template strand.

[c] P is the base on the primer strand.

[d] Yellow highlighted number denotes a disruption.

Table S6. Hydrogen bond occupancies (%) of minor groove contacts.

[BP]G* at Pre-insertion Site of Open BF (Step 1)				
Donor	Acceptor	control	*anti*-[BP]G*	*syn*-[BP]G*
Gln-797 Nε2 [a]	G (T1 [c]) N3	30.0	44.8	23.0
Arg-615 Nη1 [b]	C (P1 [d]) O^2	92.5	75.0	93.1

[BP]G* at Insertion Site of Closed BF (Step 2)							
Donor	Acceptor	control	*anti*-[BP]G* :dCTP	*syn*-[BP]G*: dATP	*syn*-[BP]G*: dCTP	*syn*-[BP]G*: dGTP	*syn*-[BP]G*: dTTP
Gln-797 Nε2	G (T1) N3	29.4	1.3 [e]	22.2	18.8	32.0	29.1
Arg-615 Nη1	C (P1) O^2	99.4	99.2	97.2	69.8	99.6	100.0

[BP]G* at Post-insertion Site of Open BF (Step 3)									
Donor	Acceptor	control	*anti*-1-[BP]G*:dC	*anti*-2-[BP]G*:dC	*anti*-3-[BP]G*:dC	*syn*-[BP]G*: dA	*syn*-[BP]G*: dC	*syn*-[BP]G*: dG	*syn*-[BP]G*: dT
Gln-797 Nε2	[BP]G* (T1) N3	22.5	0	0	0	0	0	0	0
Arg-615 Nη1	N [f] (P1) O^2/N3	96.9	0	0	0	89.7	94.6	70.1	95.1

[BP]G* at Post-insertion Site of Closed BF (Step 4)							
Donor	Acceptor	control	*anti*-[BP]G*:dC	*syn*-[BP]G*: dA	*syn*-[BP]G*: dC	*syn*-[BP]G*: dG	*syn*-[BP]G*: dT
Gln-797 Nε2	[BP]G* (T1) N3	40.5	0	0	0	0	0
Arg-615 Nη1	N (P1) O^2/N3	99.4	0	99.5	94.6	85.1	91.1

[a] % occupied indicates percentage of the time (time range, 0.8-2 ns) that the hydrogen bond was intact. Hydrogen bonding criteria were 3.3 Å between heavy atoms and a hydrogen bonding angle of 120º, as in the crystal structure (PDB ID: 1XC9) [18].

[b] % occupied indicates percentage of the time (time range, 0.8-2 ns) that the hydrogen bond was intact. Hydrogen bonding criteria were 3.3 Å between heavy atoms and a hydrogen bonding angle of 135º.

[c] T1 is the +1 base on the template strand.

[d] P1 is the +1 base on the primer strand.

[e] Yellow highlighted number denotes a disruption.

[f] N=A/C/G/T

Table S7. Post-insertion site width (Å) [a].

[BP]G* at pre-insertion site of open BF (Step 1)		
control	*anti*-[BP]G*	*syn*-[BP]G*
10.9±0.2	10.6±0.2	10.5±0.2

[BP]G* at Insertion Site of Closed BF (Step 2)					
control	*anti*-[BP]G*: dCTP	*syn*-[BP]G*: dATP	*syn*-[BP]G*: dCTP	*syn*-[BP]G*: dGTP	*syn*-[BP]G*: dTTP
10.9±0.2	10.9±0.2	10.8±0.2	10.5±0.4	10.8±0.2	10.9±0.2

[BP]G* at Post-insertion Site of Open BF (Step 3)							
control	*anti*-1-[BP]G*:dC	*anti*-2-[BP]G*:dC	*anti*-3-[BP]G*:dC	*syn*-[BP]G*:dA	*syn*-[BP]G*:dC	*syn*-[BP]G*:dG	*syn*-[BP]G*:dT
10.7±0.2	10.6±0.1	10.6±0.2	10.7±0.2	10.1±0.3	10.4±0.6	10.1±0.3	10.0±0.4

[BP]G* at Post-insertion Site of Closed BF (Step 4)					
control	*anti*-[BP]G*:dC	*syn*-[BP]G*:dA	*syn*-[BP]G*:dC	*syn*-[BP]G*:dG	*syn*-[BP]G*:dT
10.8±0.2	12.1±0.4 [b]	10.2±0.3	10.4±0.3	11.9±0.2	9.5±0.2

[a] Ensemble average values and standard deviations are provided.

[b] Yellow highlighted number denotes a disruption.

Table S8. Hydrogen bond occupancies (%)[a] involving the incoming dNTP and the polymerase in closed BF.

[BP]G* at Insertion Site of Closed BF (Step 2)

Donor	Acceptor	control	*anti*-[BP]G*:dCTP	*syn*-[BP]G*:dATP	*syn*-[BP]G*:dCTP	*syn*-[BP]G*:dGTP	*syn*-[BP]G*:dTTP	Identified in crystal?
Glu-658 N	dNTP O3'	67.8	86.2	40.2	96.7	68.6	80.0	yes
Lys706 Nξ	dNTP O1α	99.1	97.8	98.8	96.7	75.7	96.6	yes
Lys-706 Nξ	dNTP O3α	31.6	25.8	33.2	16.9	10.7	32.6	yes
Gln-656 N	dNTP O3β	80.3	96.0	92.8	69.4	96.7	90.0	no
Lys-706 Nξ	dNTP O1γ	90.5	100.0	99.0	97.8	30.4 [b]	96.1	yes
Arg-702 Nη1	dNTP O1γ	100.0	100.0	100.0	99.7	100.0	99.9	yes
Arg-702 Nη2	dNTP O3γ	100.0	99.9	99.8	95.4	99.4	99.9	yes

[BP]G* at Post-insertion Site of Closed BF (Step 4)

Donor	Acceptor	control	*anti*-[BP]G*:dC	*syn*-[BP]G*:dA	*syn*-[BP]G*:dC	*syn*-[BP]G*:dG	*syn*-[BP]G*:dT	Identified in crystal?
Glu-658 N	dGTP O3'	52.0	0	37.4	65.1	61.8	63.8	yes
Lys-706 Nξ	dGTP O1α	99.7	98.2	99.2	98.7	99.4	99.7	yes
Lys-706 Nξ	dGTP O3α	18.9	23.8	16.9	20.5	25.4	27.3	yes
Gln-656 N	dGTP O3β	99.8	90.9	97.4	95.2	96.9	94.9	no
Lys-706 Nξ	dGTP O1γ	99.6	99.6	66.5	74.5	99.2	99.2	yes
Arg-702 Nη1	dGTP O1γ	100.0	100.0	100.0	100.0	100.0	100.0	yes
Arg-702 Nη2	dGTP O3γ	99.8	98.8	100.0	100.0	100.0	100.0	yes

[a] % occupied indicates percentage of the time (time range, 0.8-2 ns) that the hydrogen bond was intact. Hydrogen bonding criteria were 3.3 Å between heavy atoms and a hydrogen bonding angle of 135º.

[b] Yellow highlighted number denotes a disruption.

Table S9. Width and height (template and primer sides) of active site in closed BF (Å) [a].

[BP]G* at Insertion Site of Closed BF (Step 2)						
Model	control	*anti*-[BP]G*:dCTP	*syn*-[BP]G*:dATP	*syn*-[BP]G*:dCTP	*syn*-[BP]G*:dGTP	*syn*-[BP]G*:dTTP
[BP]G* (T) [b] C1'-dNTP C1'	10.7±0.1	10.5±0.2	11.0±0.2	11.0±0.3	11.3±0.2	11.4±0.3
Phe-710 Cα-G (T) C6	8.1±0.3	9.4±0.6	8.2±0.3	9.0±0.3	8.5±0.3	7.5±0.4
Lys-706 Cα-C (P) [c] C6	9.1±0.3	9.2±0.4	9.9±0.3	9.0±0.4	9.4±0.3	9.7±0.3
[BP]G* atPost-insertion Site of Closed BF (Step 4)						
Model	control	*anti*-[BP]G*:dC	*syn*-[BP]G*:dA	*syn*-[BP]G*:dC	*syn*-[BP]G*:dG	*syn*-[BP]G*:dT
C (T) C1'-dGTP C1'	10.7±0.1	10.9±0.2	10.7±0.1	10.7±0.2	10.8±0.2	10.7±0.1
Phe-710 Cα-[BP]G* (T) C6	8.2±0.3	8.0±0.3	10.5±0.3 [d]	10.4±0.3	8.1±0.3	10.0±0.3
Lys-706 Cα-N [e] (P) C6	9.1±0.3	9.8±0.6	9.8±0.3	10.7±0.4	8.9±0.5	9.1±0.3

[a] Ensemble average values and standard deviations are provided.

[b] T1 is the +1 base on the template strand.

[c] P1 is the +1 base on the primer strand.

[d] Yellow highlighted number denotes a disruption.

[e] N=A/C/G/T

Table S10. Occupancies of near reaction-ready distances in the range of 3.1-3.5 Å (%)[a] and ensemble average of the attacking angle (º)[b].

[BP]G* at Insertion Site of Closed BF (Step 2)						
models	control	*anti*-[BP]G*: dCTP	*syn*-[BP]G*: dATP	*syn*-[BP]G*: dCTP	*syn*-[BP]G*: dGTP	*syn*-[BP]G*: dTTP
Distance Occupancy (%)	33.3	56.7	59.3	65.6	54.2	42.5
Angle (º)	163.4±5.9	169.3±5.7	164.8±4.8	169.4±5.0	169.5±4.6	164.8±5.7
[BP]G* at Post-insertion Site of Closed BF (Step 4)						
models	control	*anti*-[BP]G*:dC	*syn*-[BP]G*:dA	*syn*-[BP]G*:dC	*syn*-[BP]G*:dG	*syn*-[BP]G*:dT
Distance Occupancy (%)	45.8	63.9	52.3	35.6	50.8	53.0
Angle (º)	170.4±4.3	169.1±4.8	169.2±4.4	171.4±4.3	169.8±4.4	169.3±4.3

[a] % occupied indicates the percentage of the time (time range, 0.8-2 ns) that the hydrogen bond was intact. Hydrogen bonding criteria were 3.3 Å between heavy atoms and a hydrogen bonding angle of 135º.

[b] Ensemble average values and standard deviations are provided.

Table S11. Average distances (Å)[a] between Mg^{2+} and chelating residues and between the two Mg^{2+} ions in closed BF.

[BP]G* at Insertion Site of Closed BF (Step 2)						
models	control	*anti*-[BP]G*:dCTP	*syn*-[BP]G*:dATP	*syn*-[BP]G*:dCTP	*syn*-[BP]G*:dGTP	*syn*-[BP]G*:dTTP
MgA-3'O	2.2±0.1	2.1±0.1	2.1±0.1	2.1±0.1	2.2±0.2	2.2±0.1
MgA-Oδ2 of Asp 653	1.9±0.0	1.9±0.0	1.9±0.0	1.9±0.0	1.9±0.0	1.9±0.0
MgA-Oδ1 of Asp 830	1.9±0.0	1.9±0.0	1.9±0.0	1.9±0.0	1.9±0.0	1.9±0.0
MgA-Oε2 of Glu 831	1.9±0.0	1.9±0.0	1.9±0.0	1.8±0.0	1.9±0.0	1.9±0.0
MgA-Oα of dNTP	2.0±0.1	2.2±0.3	2.0±0.1	2.5±0.3	2.0±0.1	2.0±0.2
MgA-O of a water	2.0±0.1	2.0±0.1	2.0±0.1	2.0±0.1	2.0±0.1	2.0±0.1
MgB-Oδ1 of Asp 653	1.9±0.0	1.9±0.0	1.9±0.0	1.9±0.0	1.9±0.0	1.9±0.0
MgB-O of Tyr 654	1.9±0.1	2.0±0.1	1.9±0.1	2.0±0.1	2.0±0.1	1.9±0.1
MgB-Oδ2 of Asp 830	1.9±0.0	1.9±0.0	1.9±0.0	1.9±0.0	1.9±0.0	1.9±0.0
MgB-Oα of dNTP	2.8±0.2	2.4±0.3	2.8±0.2	2.1±0.3	2.5±0.3	2.7±0.3
MgB-Oβ of dNTP	1.9±0.1	1.9±0.1	1.8±0.0	2.0±0.1	1.9±0.0	1.9±0.1
MgB-Oγ of dNTP	1.8±0.0	1.8±0.0	1.8±0.0	1.8±0.0	1.8±0.0	1.8±0.0
MgA-MgB	3.8±0.1	3.7±0.1	3.8±0.1	3.8±0.1	3.7±0.1	3.8±0.1
[BP]G* at Post-insertion Site of Closed BF (Step 4)						
models	control	*anti*-[BP]G*:dC	*syn*-[BP]G*:dA	*syn*-[BP]G*:dC	*syn*-[BP]G*:dG	*syn*-[BP]G*:dT
MgA-3'O	2.1±0.1	2.1±0.1	2.2±0.2	2.1±0.1	2.1±0.1	2.2±0.1
MgA-Oδ2 of Asp 653	1.9±0.0	1.9±0.0	1.9±0.0	1.9±0.0	1.9±0.0	1.9±0.0
MgA-Oδ1 of Asp 830	1.9±0.0	1.9±0.0	1.9±0.0	1.9±0.0	1.9±0.0	1.9±0.0
MgA-Oε2 of Glu 831	1.9±0.0	1.9±0.0	1.9±0.0	1.9±0.0	1.9±0.0	1.9±0.0
MgA-Oα of dNTP	2.3±0.2	2.3±0.3	2.0±0.1	2.1±0.2	2.2±0.2	2.0±0.1
MgA-O of a water	2.0±0.1	2.0±0.1	2.0±0.1	2.0±0.1	2.0±0.1	2.0±0.1
MgB-Oδ1 of Asp 653	1.9±0.0	1.9±0.0	1.9±0.0	1.9±0.1	1.9±0.0	1.9±0.0
MgB-O of Tyr 654	2.0±0.1	2.0±0.1	2.0±0.1	2.0±0.1	2.0±0.1	2.0±0.1
MgB-Oδ2 of Asp 830	1.9±0.1	1.9±0.1	1.9±0.0	1.9±0.0	1.9±0.0	1.9±0.0
MgB-Oα of dNTP	2.1±0.1	2.1±0.2	2.5±0.2	2.2±0.2	2.2±0.2	2.4±0.3
MgB-Oβ of dNTP	1.9±0.0	1.9±0.0	1.9±0.0	1.9±0.0	1.9±0.0	1.9±0.0
MgB-Oγ of dNTP	1.9±0.0	1.9±0.0	1.8±0.0	1.8±0.0	1.8±0.0	1.8±0.0
MgA-MgB	3.6±0.1	3.7±0.1	3.7±0.1	3.6±0.1	3.7±0.1	3.7±0.1

[a] Ensemble average values and standard deviations are provided.

References

1. Case, D.A., Pearlman, D.A., Caldwell, J.W., Cheatham, T.E.I., Wang, J., Ross, W.S., Simmerling, C.L., Darden, T.A., Merz, K.M., Stanton, R.V., Cheng, A.L., Vincent, J.J., Crowley, M., Tsui, V., Gohlke, H., Radmer, R.J., Duan, Y., Pitera, J., Massova, I., Seibel, G.L., Singh, U.C., Weiner, P.K. and Kollman, P.A., *AMBER 7*. 2002, University of California, San Francisco, CA.
2. Arndt, J.W., Gong, W., Zhong, X., Showalter, A.K., Liu, J., Dunlap, C.A., Lin, Z., Paxson, C., Tsai, M.D. and Chan, M.K. (2001) Insight into the catalytic mechanism of DNA polymerase β: structures of intermediate complexes. *Biochemistry*, **40**, 5368-75.
3. Dunlap, C.A. and Tsai, M.D. (2002) Use of 2-aminopurine and tryptophan fluorescence as probes in kinetic analyses of DNA polymerase β. *Biochemistry*, **41**, 11226-35.
4. Liu, J. and Tsai, M.D. (2001) DNA polymerase β: pre-steady-state kinetic analyses of dATP α S stereoselectivity and alteration of the stereoselectivity by various metal ions and by site-directed mutagenesis. *Biochemistry*, **40**, 9014-22.
5. Wang, J., Wolf, R.M., Caldwell, J.W., Kollman, P.A. and Case, D.A. (2004) Development and testing of a general amber force field. *J. Comput. Chem.*, **25**, 1157-74.
6. Frisch, J.M., Trucks, W.G., Schlegel, B.H., Scuseria, E.G., Robb, A.M., Cheeseman, R.J., Zakrzewski, G.V., Montgomery, A.J., Stratmann, E.R., Burant, C.J., Dapprich, S., Millam, M.J., Daniels, D.A., Kudin, N.K., Strain, C.M., Farkas, O., Tomasi, J., Barone, V., Cossi, M., Cammi, R., Mennucci, B., Pomelli, C., Adamo, C., Clifford, S., Ochterski, J., Petersson, A.G., Ayala, Y.P., Cui, Q., Morokuma, K., Malick, K.D., Rabuck, D.A., Raghavachari, K., Foresman, B.J., Cioslowski, J., Ortiz, V.J., Baboul, G.A., Stefanov, B.B., Liu, G., Liashenko, A., Piskorz, P., Komaromi, I., Gomperts, R., Martin, L.R., Fox, J.D., Keith, T., Al-Laham, A.M., Peng, Y.C., Nanayakkara, A., Gonzalez, C., Challacombe, M., Gill, W.M.P., Johnson, B., Chen, W., Wong, W.M., Andres, L.J., Gonzalez, C., Head-Gordon, M., Replogle, S.E. and Pople, A.J., *Gaussian 98 (Revision A. 7)*. 1998, Gaussian, Inc.: Pittsburgh, PA.
7. Bayly, C.I., Cieplak, P., cornell, W.D. and Kollman, P.A. (1993) A well-behaved electrostatic potential based method using charge restraints for deriving atomic charges-The Resp model. *J. Phys. Chem.*, **97**, 10269-80.
8. Wu, X., Shapiro, R. and Broyde, S. (1999) Conformational analysis of the major DNA adduct derived from the food mutagen 2-amino-3-methylimidazo[4,5-f]quinoline. *Chem. Res. Toxicol.*, **12**, 895-905.
9. Perlow, R.A. and Broyde, S. (2002) Toward understanding the mutagenicity of an environmental carcinogen: structural insights into nucleotide incorporation preferences. *J. Mol. Biol.*, **322**, 291-309.
10. Cheatham, T.E., 3rd, Cieplak, P. and Kollman, P.A. (1999) A modified version of the Cornell *et al*. force field with improved sugar pucker phases and helical repeat. *J. Biomol. Struct. Dyn.*, **16**, 845-62.
11. Cornell, W., Cieplak, P., Bayly, C., Gould, I., Merz, K., Ferguson, D., Spellmeyer, D., Fox, T., Caldwell, J. and Kollman, P. (1995) A second generation force field for the simulation of proteins, nucleic acids, and organic molecules. *J. Am. Chem. Soc.*, **117**, 5179-97.
12. Darden, T., York, D. and Pedersen, L. (1993) Particle mesh Ewald: an N log(N) method for Ewald sums in large systems. *J. Chem. Phys.*, **98**, 10089-92.
13. Essmann, U., Perera, L., Berkowitz, M.L., Darden, T., Lee, H. and Pederson, L.G. (1995) A smooth particle mesh Ewald method. *J. Chem. Phys.*, **103**, 8577-93.
14. Ryckaert, J.P., Ciccotti, G. and Berendsen, H.J.C. (1977) Numerical integration of Cartesian equations of motion of a system with constraints: Molecular dynamics of n-alkanes. *J. Comp. Phys.*, **23**, 327-341.
15. Jorgensen, W., Chandrasekhar, J., Madura, J., Impey, R. and Klein, M. (1983) Comparison of simple potential functions for simulating liquid water. *J. Chem. Phys.*, **79**, 926-935.
16. Mezei, M. (1997) Optimal position of solute for simulations. *J. Comp. Chem.*, **18**, 812-815.

17. Berendsen, H.J.C., Postma, J.P.M., van Gunsteren, W.F., DiNola, A. and Haak, J.R. (1984) Molecular dynamics with coupling to an external bath. *J. Chem. Phys.*, **81**, 3684-90.
18. Hsu, G.W., Huang, X., Luneva, N.P., Geacintov, N.E. and Beese, L.S. (2005) Structure of a high fidelity DNA polymerase bound to a benzo[*a*]pyrene adduct that blocks replication. *J. Biol. Chem.*, **280**, 3764-70.

Scoring Criteria for Table 1:

Pre-insertion Site Pocket: a score of -1 denotes an increase in the distance compared to the control by more than 1 Å. See Table S4 for details.

Base Pair Hydrogen Bonding Geometry: a score of -1 denotes a decrease in occupancy compared to the control by more than 30%, or a loss of one hydrogen bond. See Table S5 for details.

Stacking Interaction: a score of -1 denotes a severe disruption of the stacking interaction or two diminished stacking interactions. See Figure 4 for details.

Minor Groove Contact: a score of -2 denotes a disruption of one minor groove contact [either a very low hydrogen bond occupancy (less than 2%) or a loss of one hydrogen bond]. See Table S6 for details.

Post-insertion Site Width: a score of -1 denotes an increase or a decrease in the distance compared to the control by more than 1 Å. See Table S7 for details.

Nucleotide Binding Pocket: a score of -5 denotes blocking of the nucleotide binding pocket. See Figure 6 for details.

Protein-dNTP Interactions: a score of -1 denotes a decrease in occupancy compared to the control by more than 50%, or a loss of one hydrogen bond. See Table S8 for details.

Active Site Pocket: a score of -1 denotes an increase in distances compared to the control by more than 1 Å, or a displacement by BP of one of the four amino acids comprising the pocket wall. See Table S9 and Figure 5 for details.

Pα-O3': no disruption of the near reaction ready distance is observed (a decrease in the distance occupancy compared to the control by more than 30% is considered to be a disruption). See Table S10 for details.

Attack Angle: no disruption of the attack angle is observed (a decrease compared to the control by more than 10º is considered to be a disruption). See Table S10 for details.

Mg^{2+} ions coordination: no disruptions of the chelating interactions involving the two Mg^{2+} ions are observed (an increase in any of the distances compared to the control by more than 0.5 Å is considered to be a disruption). See Table S11 for details.

Mg^{2+} ions Distance: no disruptions of the distance between the two Mg^{2+} ions are observed (an increase in the distance compared to the control by more than 0.5 Å is considered to be a disruption). See Table S11 for details.

Figure S1: Modeled geometry of the octahedral coordination of the two Mg^{2+} ions.

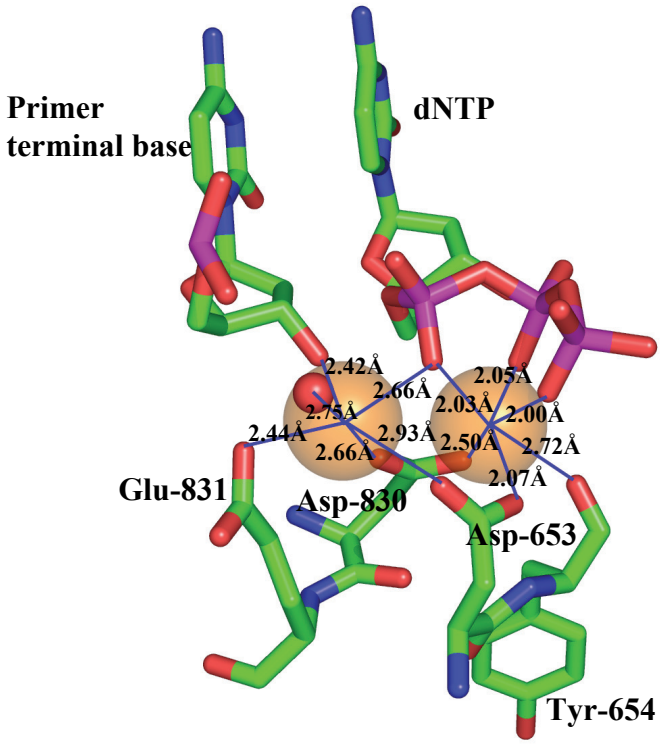

Figure S2: Stereoviews of the initial models. All stereo figures were made for viewing with a stereoviewer. The color code is the same as in Figure 5 except that the protein is shown in darker pink and the O and O1 helices are shown in magenta.

Step 1: [BP]G* at the Pre-insertion Site of Open BF

(a) control

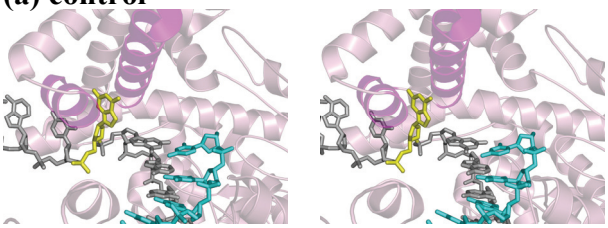

(b) *anti*-[BP]G*

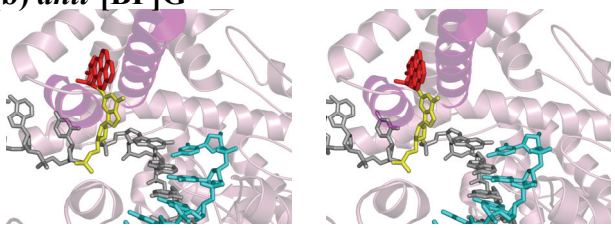

(c) *syn*-[BP]G*

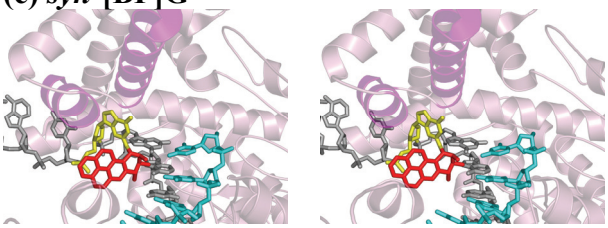

Step 2: [BP]G* at the Insertion Site of Closed BF

(d) control

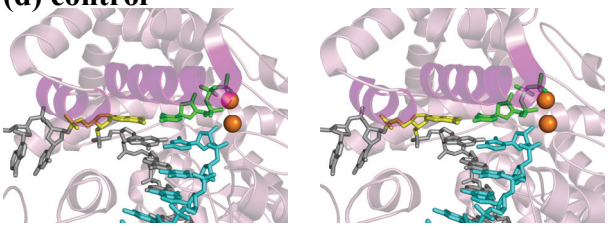

(e) *anti*-[BP]G*:dCTP

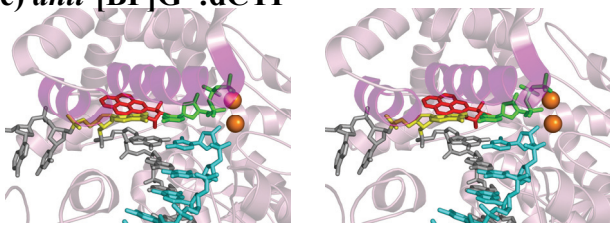

(f) *syn*-[BP]G*:dATP

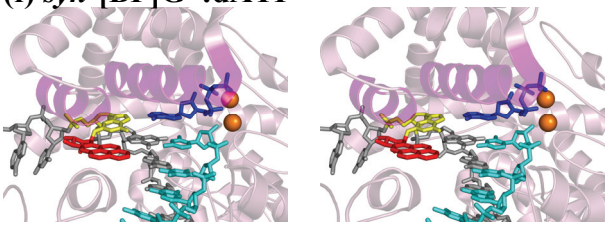

(g) *syn*-[BP]G*:dCTP

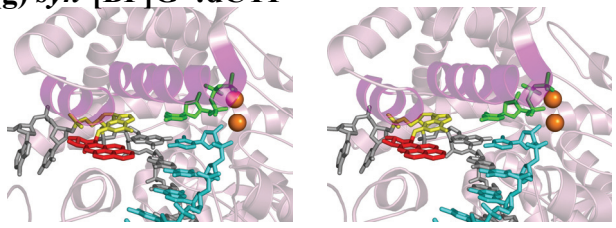

(h) *syn*-[BP]G*:dGTP

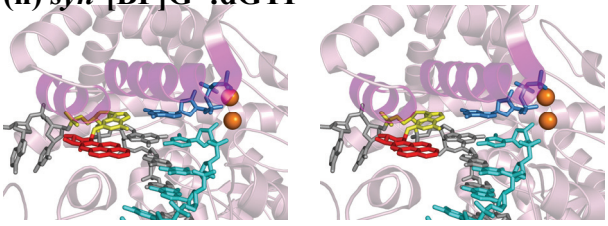

(i) *syn*-[BP]G*:dTTP

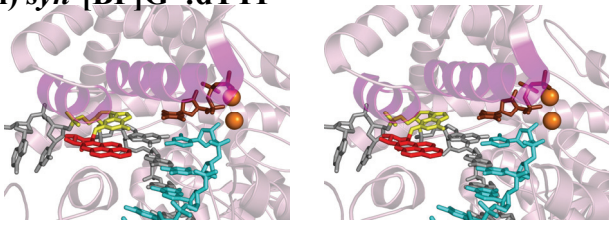

Step 3: [BP]G* at the Post-insertion Site of Open BF

(j) control

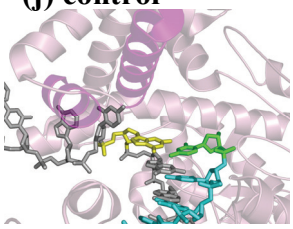

(k) *anti*-1-[BP]G*:dC

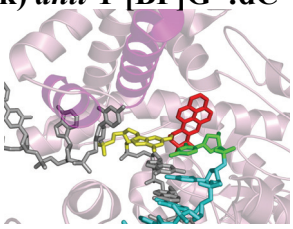

(l) *anti*-2-[BP]G*:dC

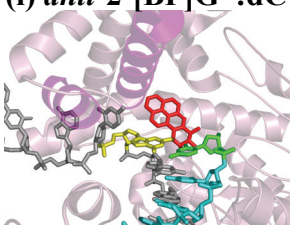

(m) *anti*-3-[BP]G*:dC

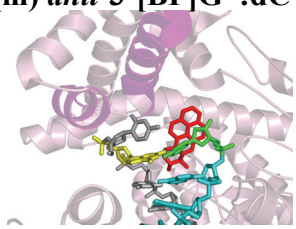

(n) *syn*-[BP]G*:dA

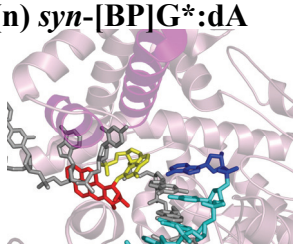

(o) *syn*-[BP]G*:dC

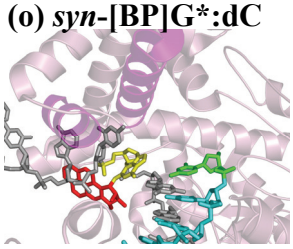

(p) *syn*-[BP]G*:dG

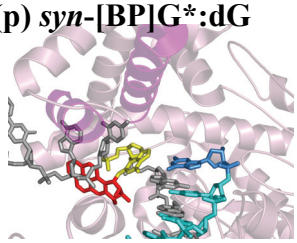

(q) *syn*-[BP]G*:dT

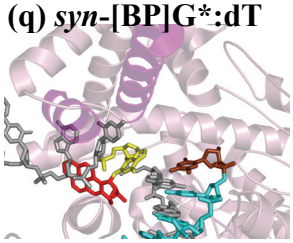

Step 4: [BP]G* at the Post-insertion Site of Closed BF

(r) control

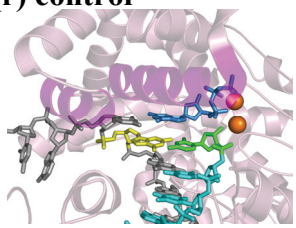

(s) *anti*-[BP]G*:dC

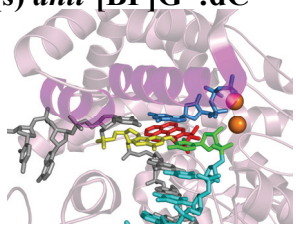

(t) *syn*-[BP]G*:dA

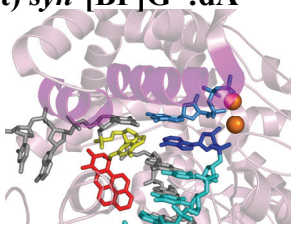

(u) *syn*-[BP]G*:dC

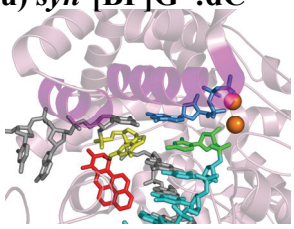

(v) *syn*-[BP]G*:dG

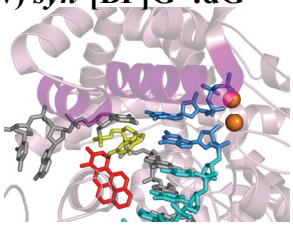

(w) *syn*-[BP]G*:dT

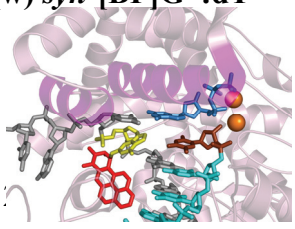

Figure S3: All-atom (red) and active-site (blue) RMSDs of each system with respect to time.

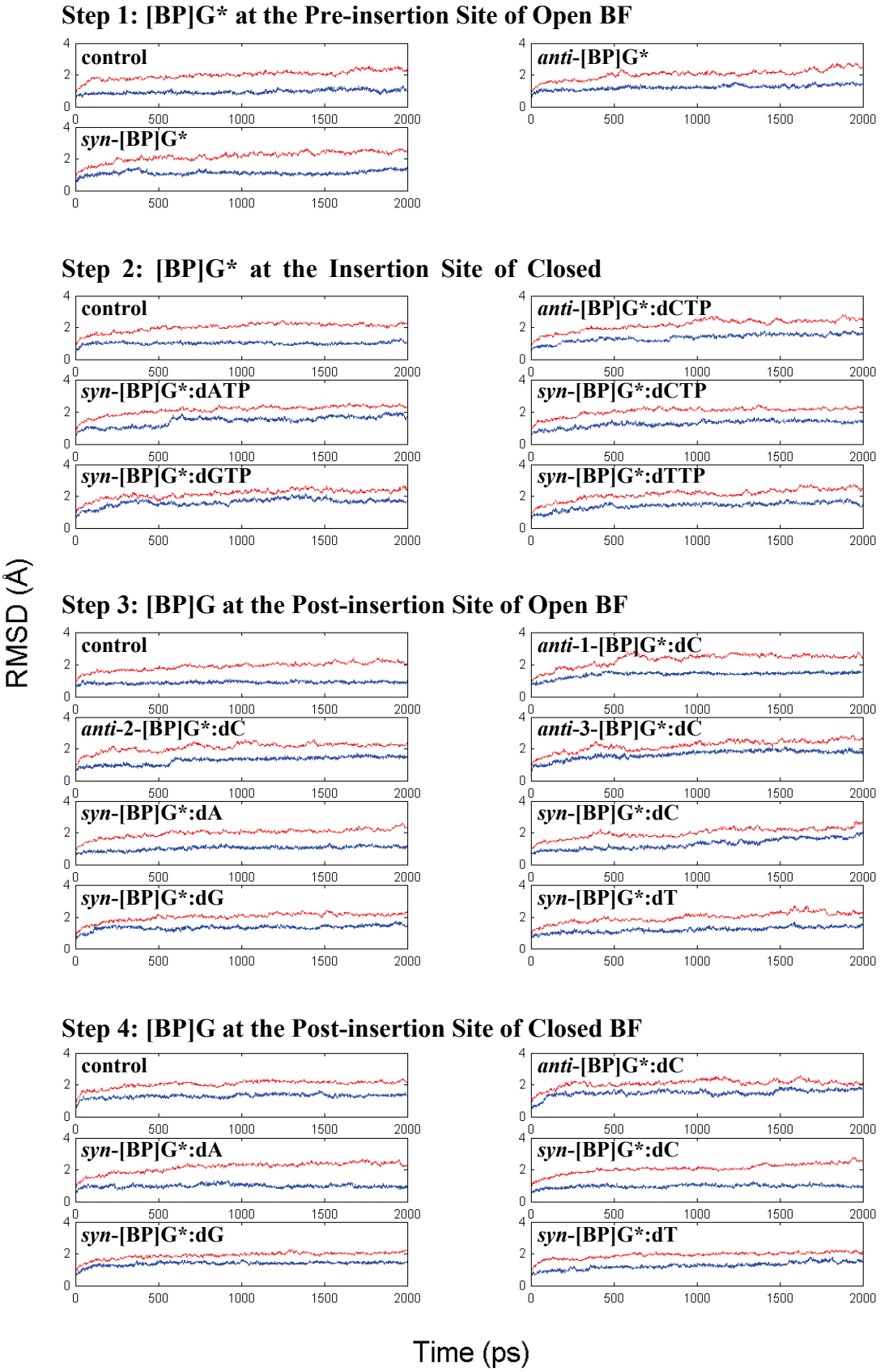

Figure S4: Determination of Michaelis-Menten parameters V_{max} and K_m for dCTP insertion opposite an unmodified guanine (CGG), and dATP or dGTP insertion opposite [BP]G* in the same CG*G sequence context, catalyzed by BF. (a) Typical polyacrylamide gel for one-step dNTP insertion. Left panel: dCTP insertion opposite the underlined G in the unmodified sequence context CGG; [DNA] = 20 nM, [BF] = 0.1 nM, incubation time = 3 min, and the dCTP concentrations are denoted for each lane (μM units). In the case of the [BP]G*–modified sequences (CG*G), the concentrations were: [DNA] = 15nM, [BF] = 2nM, incubation time = 30min, and the dATP and the dGTP concentrations are indicated in each case. Ctr shown in each panels are markers representing "-1" and "0" position. (b) Plots of the rates of dNTP incorporation, V(nM/min), as a function of the dNTP (μM) concentration. Each of the data points is the average of three experiments; the standard deviations are indicated by the error bars. The solid lines are plots of the Michaelis-Menten equation: $V = V_{max} * [dNTP]/(K_m + [dNTP])$, using values of the V_{max} and K_m shown in Table S3.

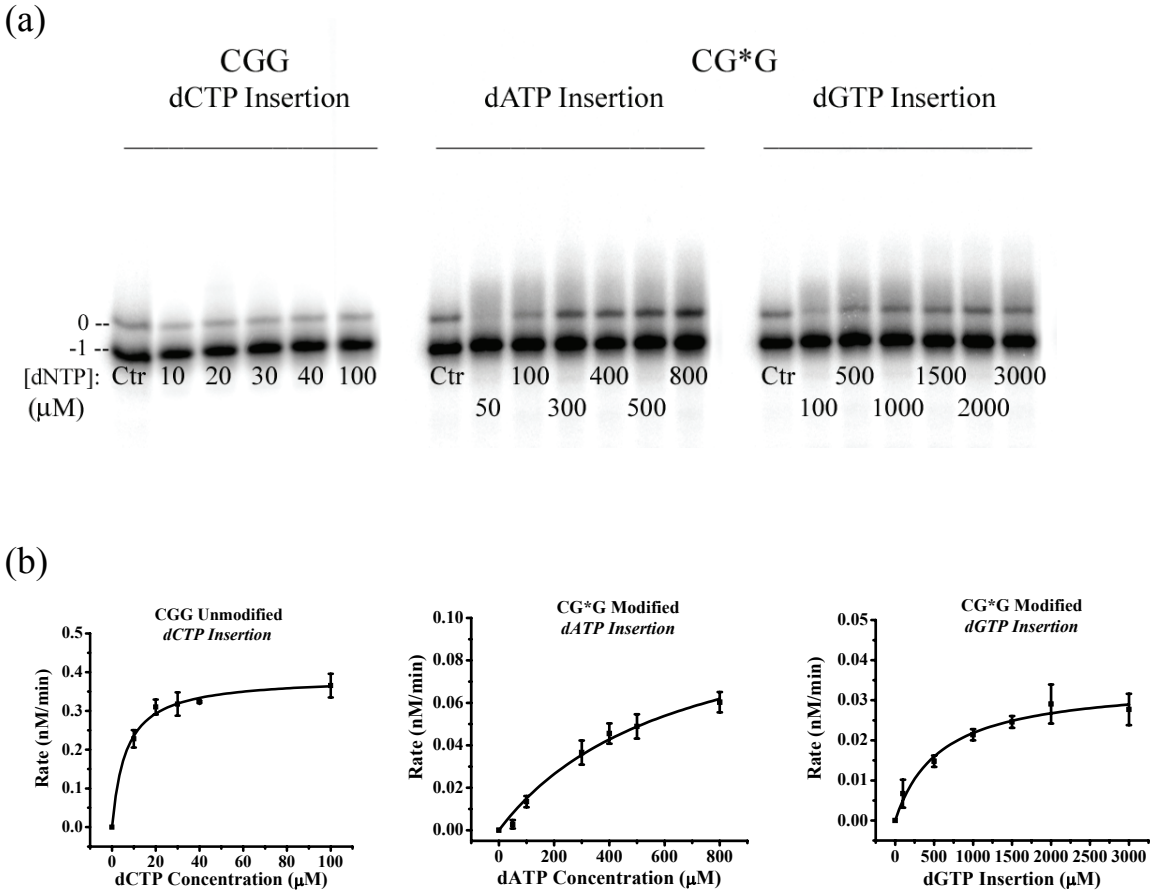

Figure S5: Stereoviews of the simulated systems (whole structure) after 2 ns MD. The color code is the same as in Figure S2.

Step 1: [BP]G* at the Pre-insertion Site of Open BF

(a) control

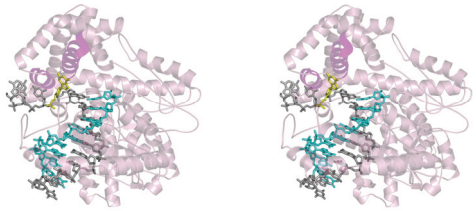

(b) *anti*-[BP]G*

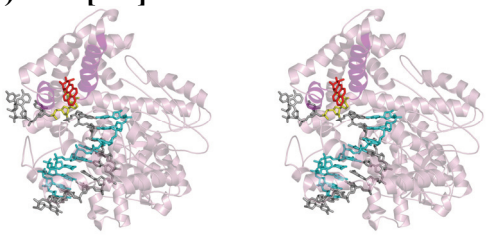

(c) *syn*-[BP]G*

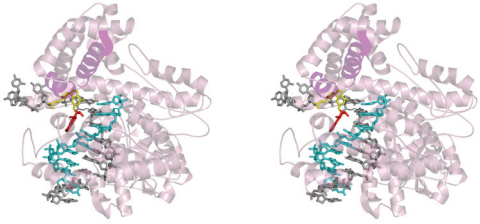

Step 2: [BP]G* at the Insertion Site of Closed BF

(d) control

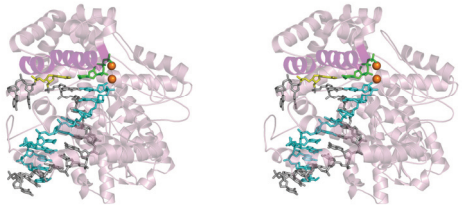

(e) *anti*-[BP]G*:dCTP

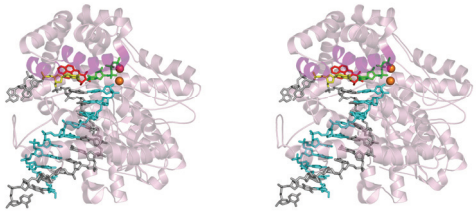

(f) *syn*-[BP]G*:dATP

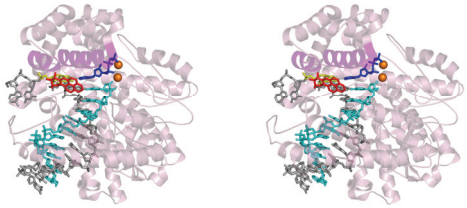

(g) *syn*-[BP]G*:dCTP

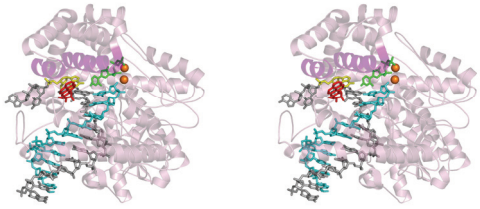

(h) *syn*-[BP]G*:dGTP

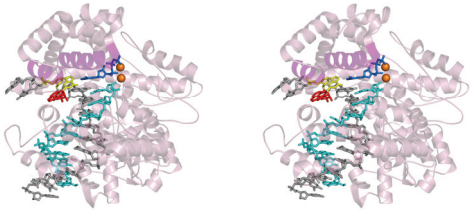

(i) *syn*-[BP]G*:dTTP

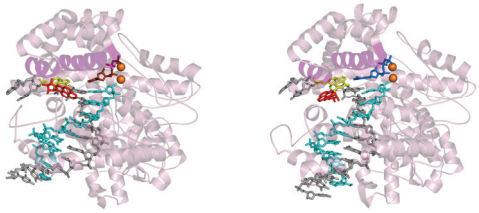

Step 3: [BP]G* at the Post-insertion Site of Open BF

(j) control

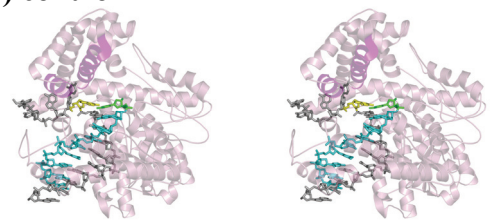

(k) *anti*-1-[BP]G*:dC

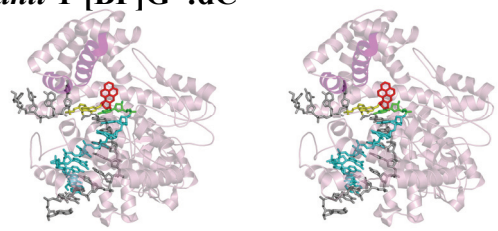

(l) *anti*-2-[BP]G*:dC

(m) *anti*-3-[BP]G*:dC

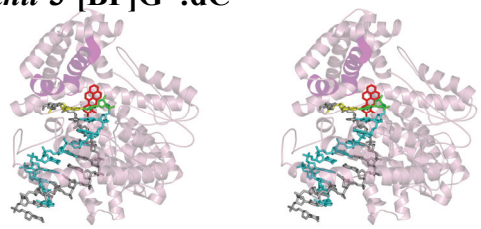

(n) *syn*-[BP]G*:dA

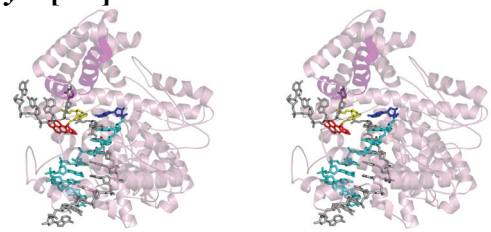

(o) *syn*-[BP]G*:dC

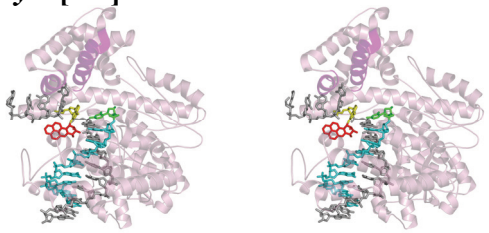

(p) *syn*-[BP]G*:dG

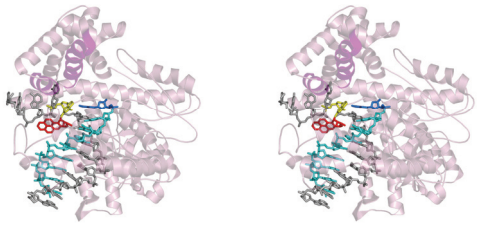

(q) *syn*-[BP]G*:dT

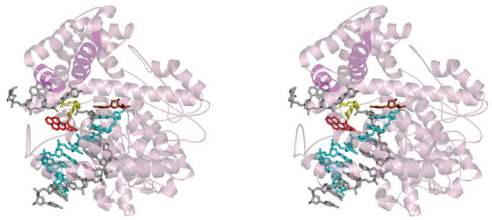

Step 4: [BP]G* at the Post-insertion Site of Closed BF

(r) control

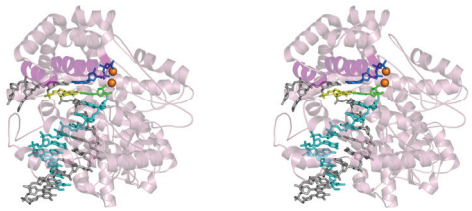

(s) *anti*-[BP]G*:dC

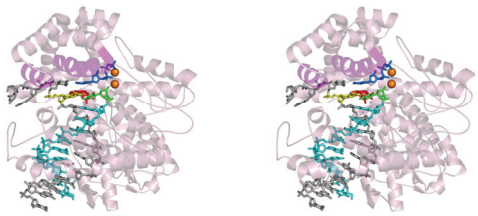

(t) *syn*-[BP]G*:dA

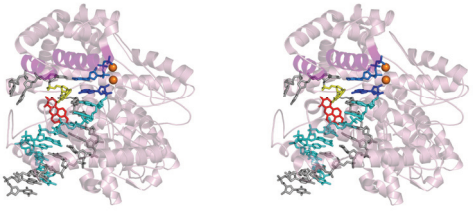

(u) *syn*-[BP]G*:dC

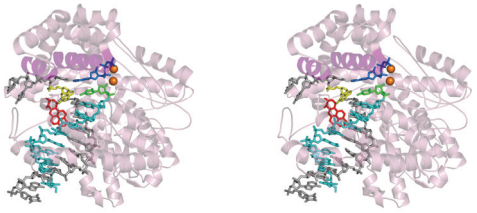

(v) *syn*-[BP]G*:dG

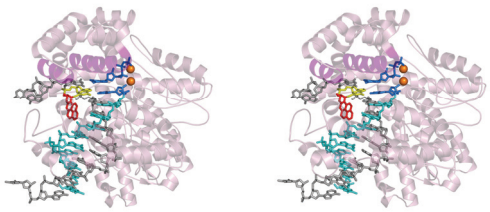

(w) *syn*-[BP]G*:dT

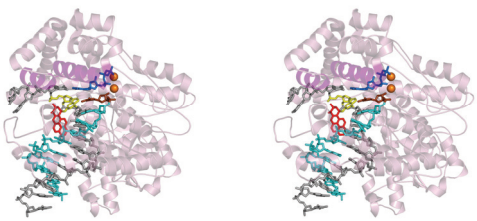

Figure S6: Stereoviews of the simulated systems (active site) after 2 ns MD. The color code is the same as in Figure S2.

Step 1: [BP]G* at the Pre-insertion Site of Open BF

(a) control

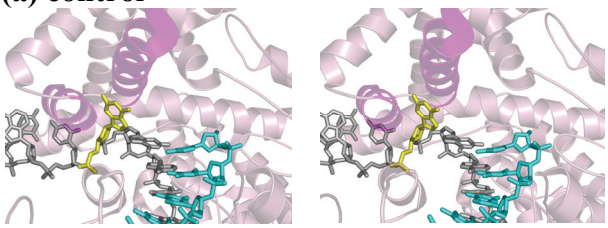

(b) *anti*-[BP]G*

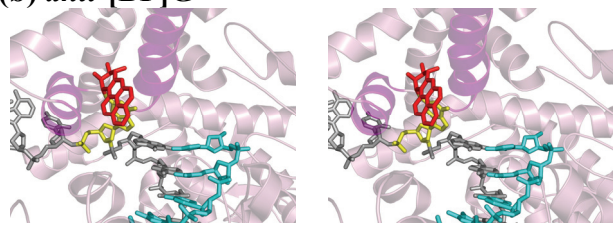

(c) *syn*-[BP]G*

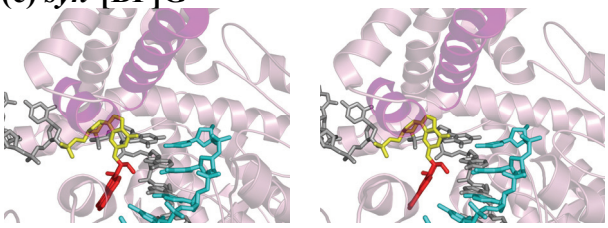

Step 2: [BP]G* at the Insertion Site of Closed BF

(d) control

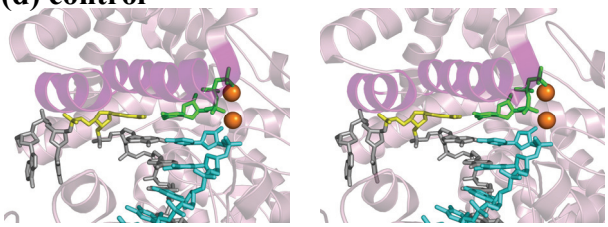

(e) *anti*-[BP]G*:dCTP

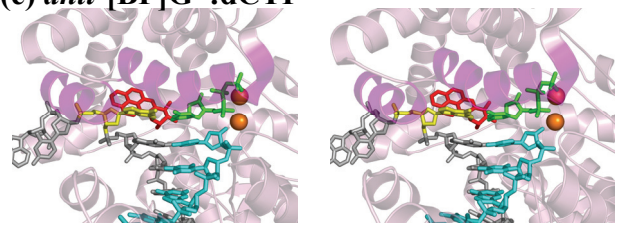

(f) *syn*-[BP]G*:dATP

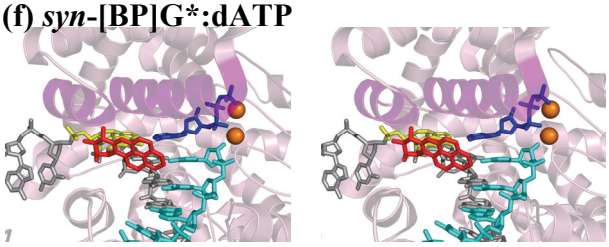

(g) *syn*-[BP]G*:dCTP

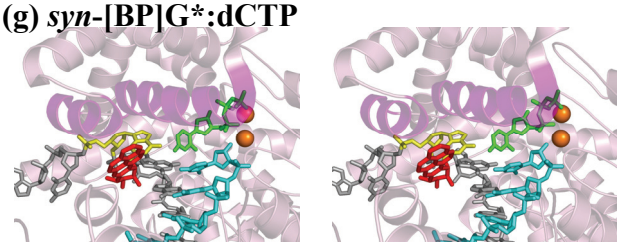

(h) *syn*-[BP]G*:dGTP

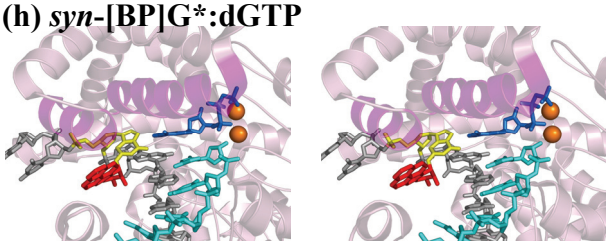

(i) *syn*-[BP]G*:dTTP

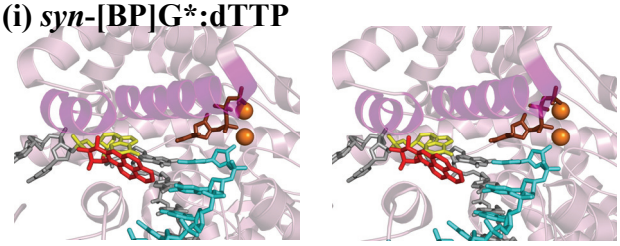

Step 3: [BP]G* at the Post-insertion Site of Open BF

(j) control

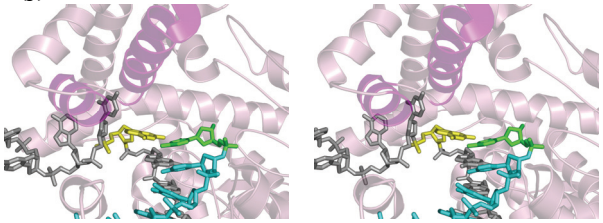

(k) *anti*-1-[BP]G*:dC

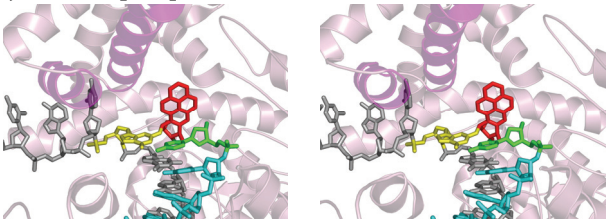

(l) *anti*-2-[BP]G*:dC

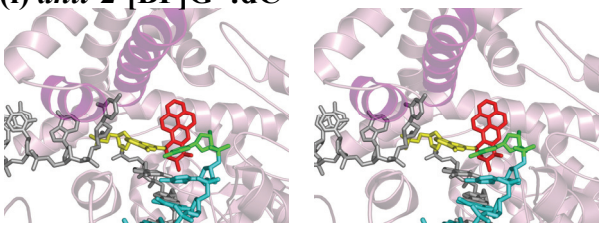

(m) *anti*-3-[BP]G*:dC

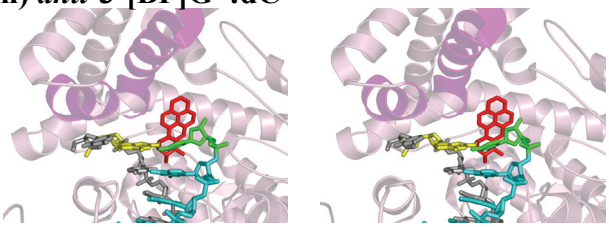

(n) *syn*-[BP]G*:dA

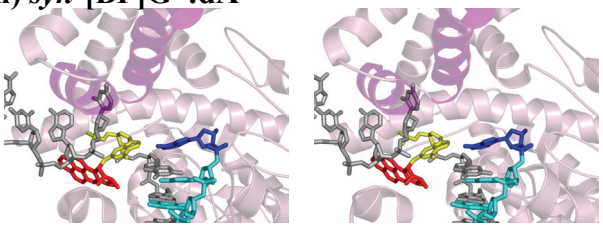

(o) *syn*-[BP]G*:dC

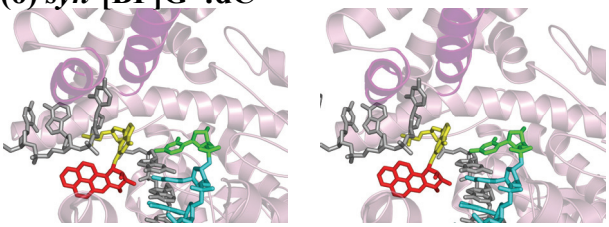

(p) *syn*-[BP]G*:dG

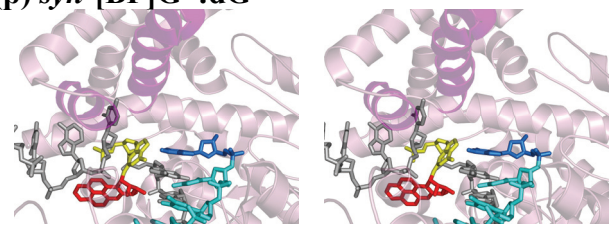

(q) *syn*-[BP]G*:dT

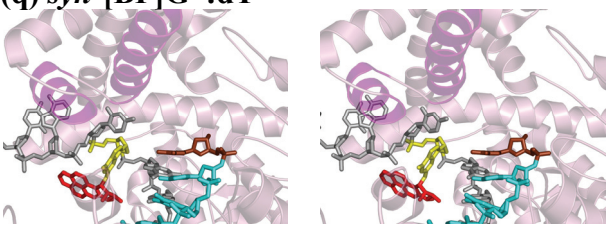

Step 4: [BP]G* at the Post-insertion Site of Closed BF

(r) control

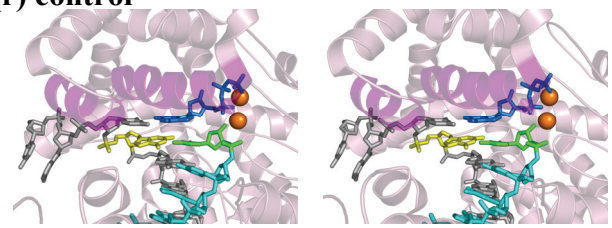

(s) *anti*-[BP]G*:dC

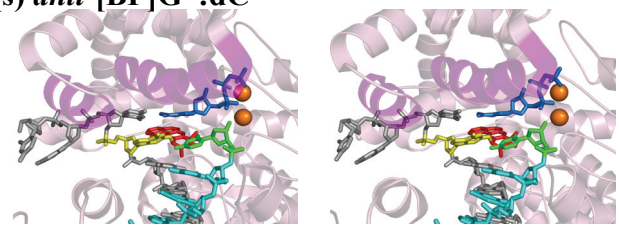

(t) *syn*-[BP]G*:dA

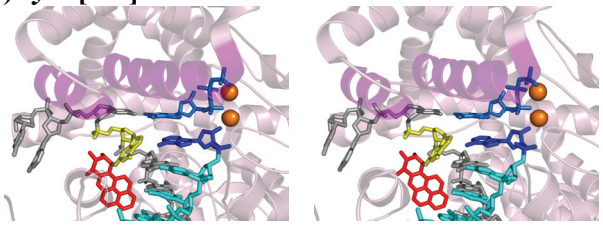

(u) *syn*-[BP]G*:dC

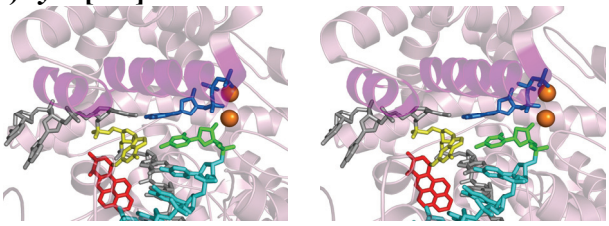

(v) *syn*-[BP]G*:dG

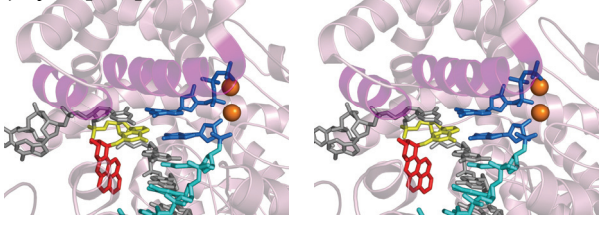

(w) *syn*-[BP]G*:dT

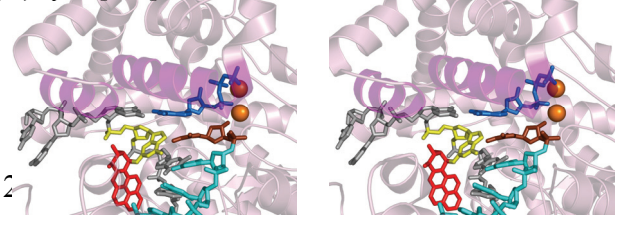

Figure S7: Width of the pre-insertion site measured by the distance between the Cα of the Gly-711 from the O helix and the Cα of the Leu-721 from the O1 helix.

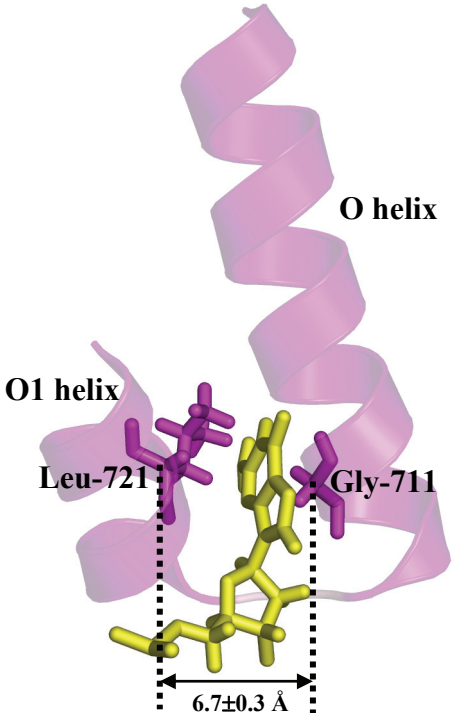

Figure S8: Hydrogen bonds between [BP]G* and different partners at Steps 2-4. Black dashed lines denote hydrogen bonds. The BP ring is shown in red.

Step 2: [BP]G* at the Insertion Site of Closed BF

(a) control

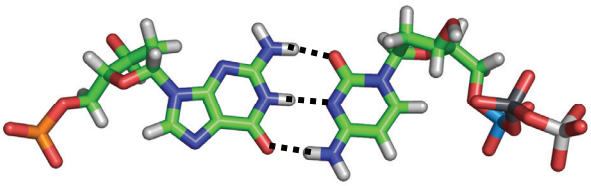

(b) *anti*-[BP]G*:dCTP

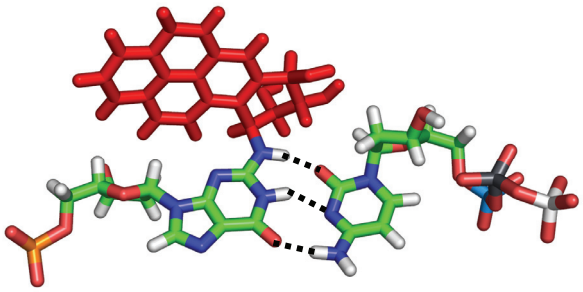

(c) *syn*-[BP]G*:dATP

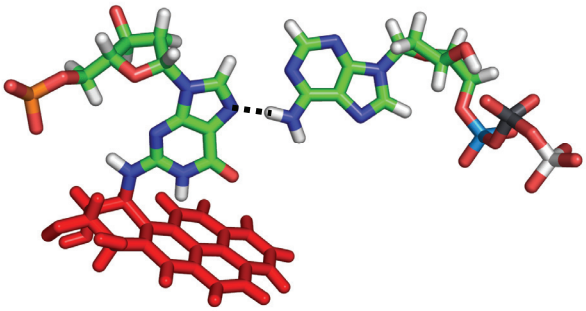

(d) *syn*-[BP]G*:dCTP

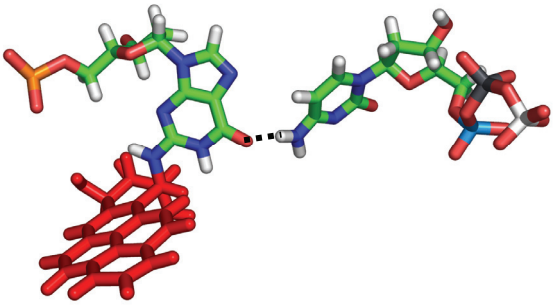

(e) *syn*-[BP]G*:dGTP

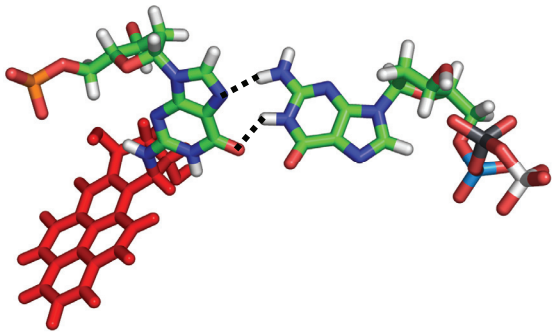

(f) *syn*-[BP]G*:dTTP

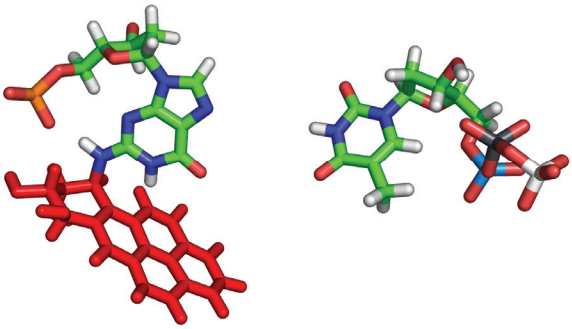

Step 3: [BP]G* at the Post-insertion Site of Open BF

(g) control

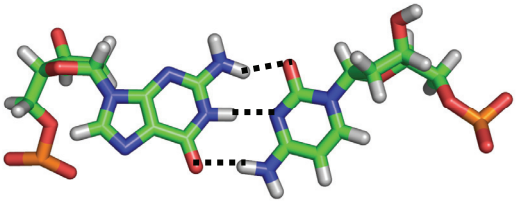

(h) *anti*-1-[BP]G*:dC

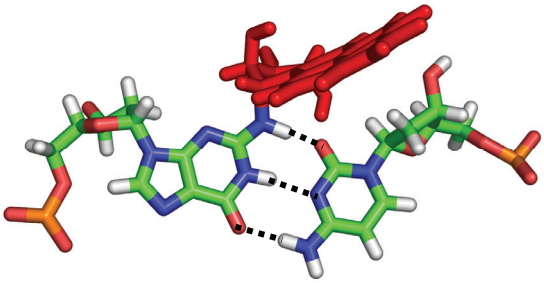

(i) *anti*-2-[BP]G*:dC

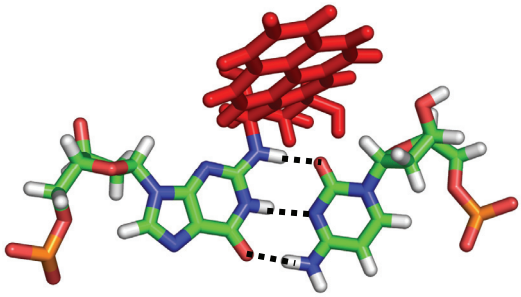

(j) *anti*-3-[BP]G*:dC

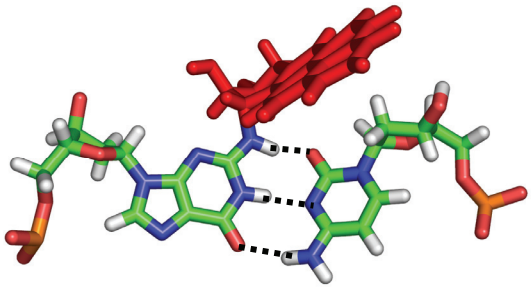

(k) *syn*-[BP]G*:dA

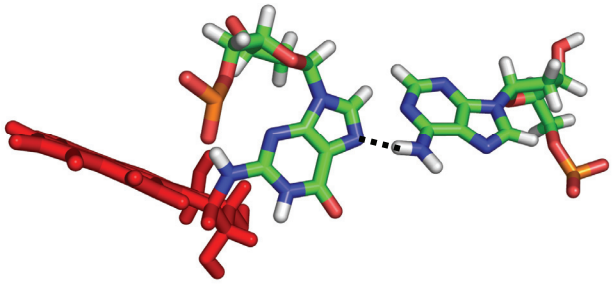

(l) *syn*-[BP]G*:dC

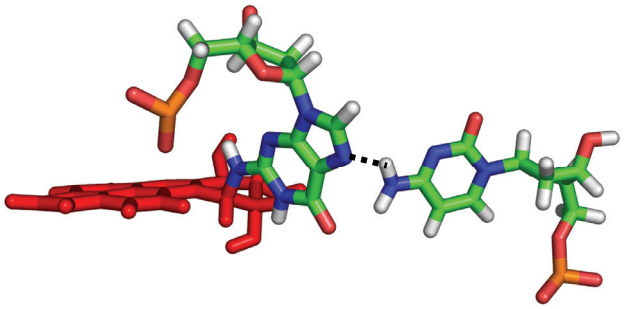

(m) *syn*-[BP]G*:dG

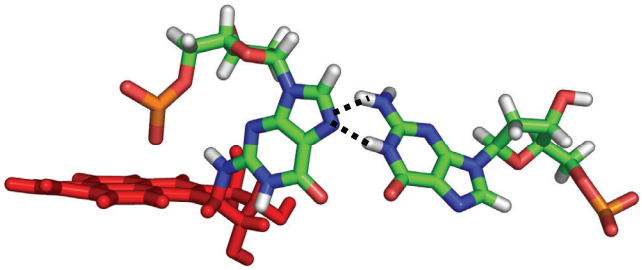

(n) *syn*-[BP]G*:dT

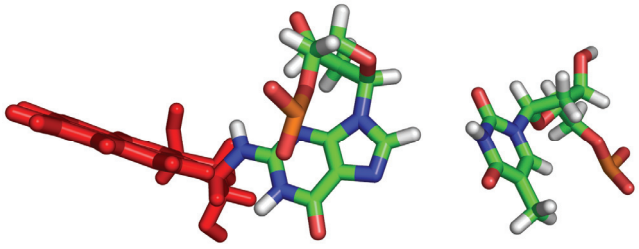

Step 4: [BP]G* at the Post-insertion Site of Closed BF

(o) control

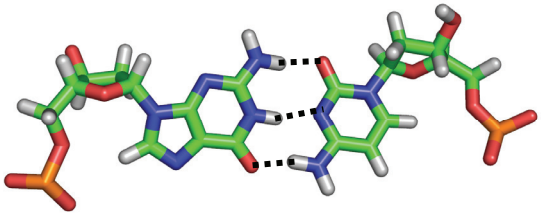

(p) *anti*-[BP]G*:dC

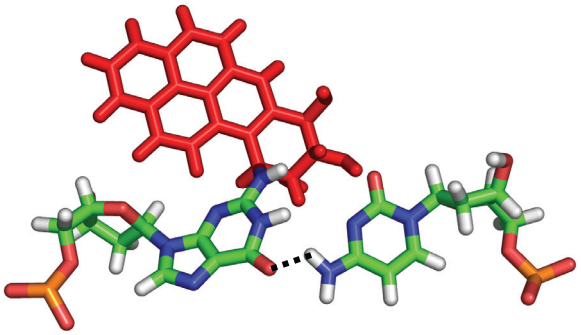

(q) *syn*-[BP]G*:dA

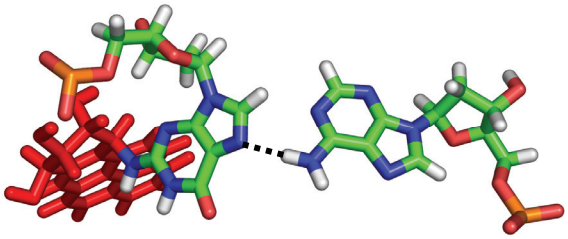

(r) *syn*-[BP]G*:dC

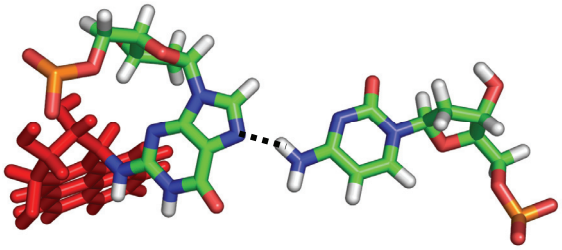

(s) *syn*-[BP]G*:dG

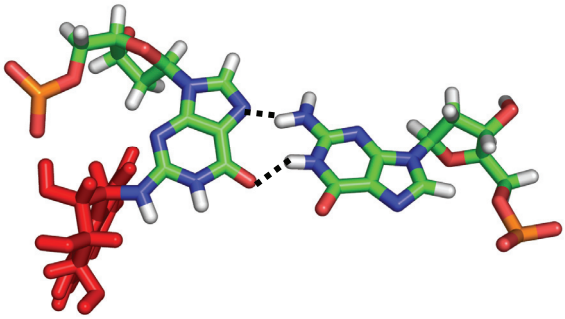

(t) *syn*-[BP]G*:dT

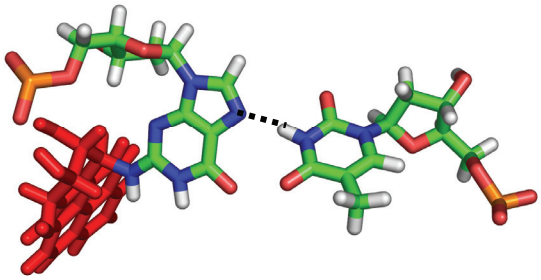

Figure S9: Time dependence of the distance between the 3'O of the primer terminus and α-phosphate of the incoming dNTP and the attacking angle in the BF closed ternary complexes. Color code: black, unmodified control; blue, *syn*-[BP]G*:dATP/dA; green, *syn*-[BP]G*:dCTP/dC; cyan, *syn*-[BP]G*:dGTP/dG; red, *syn*-[BP]G*:dTTP/dT; magenta, *anti*-[BP]G*:dCTP/dC.

Step 2: [BP]G* in the insertion site of closed BF

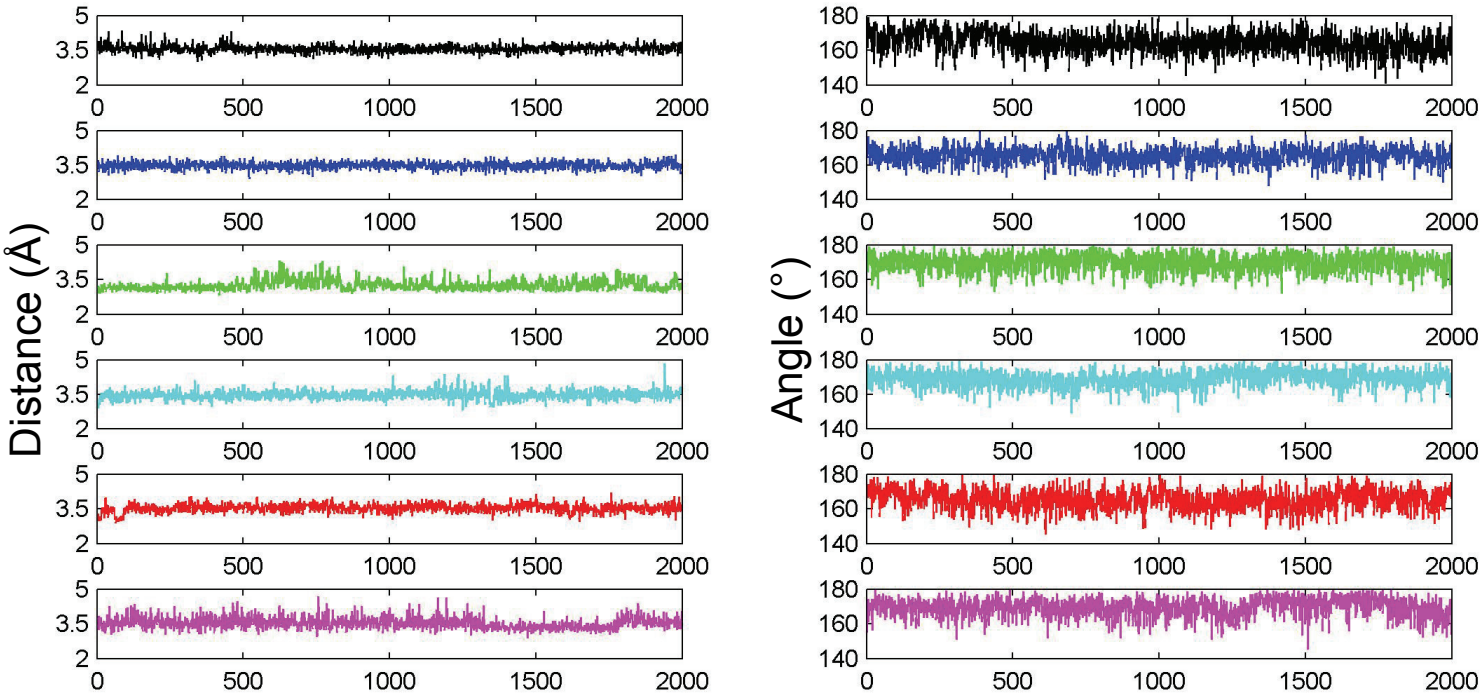

Step 4: [BP]G* in the post-insertion site of closed BF

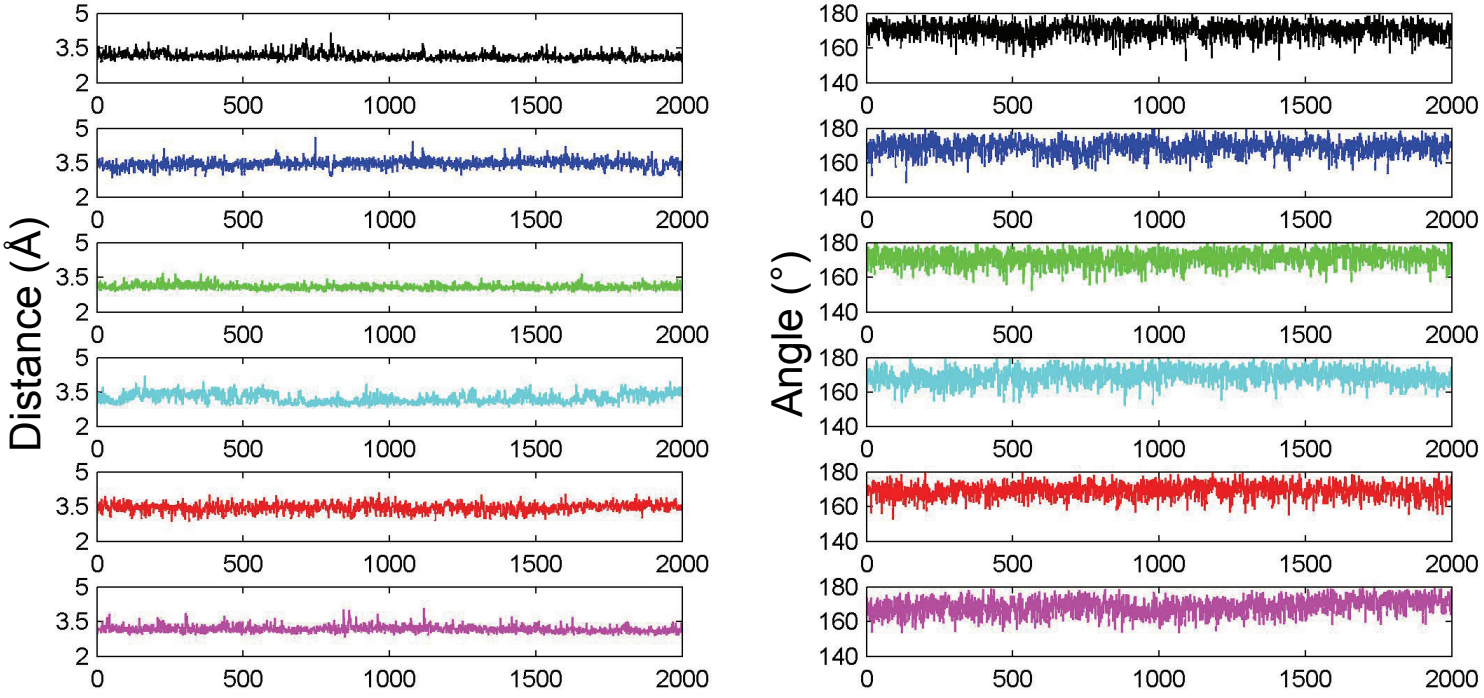

Figure S10: χ as a function of time for the primer terminal C in the *syn*-[BP]G*:dC system at Step 4.

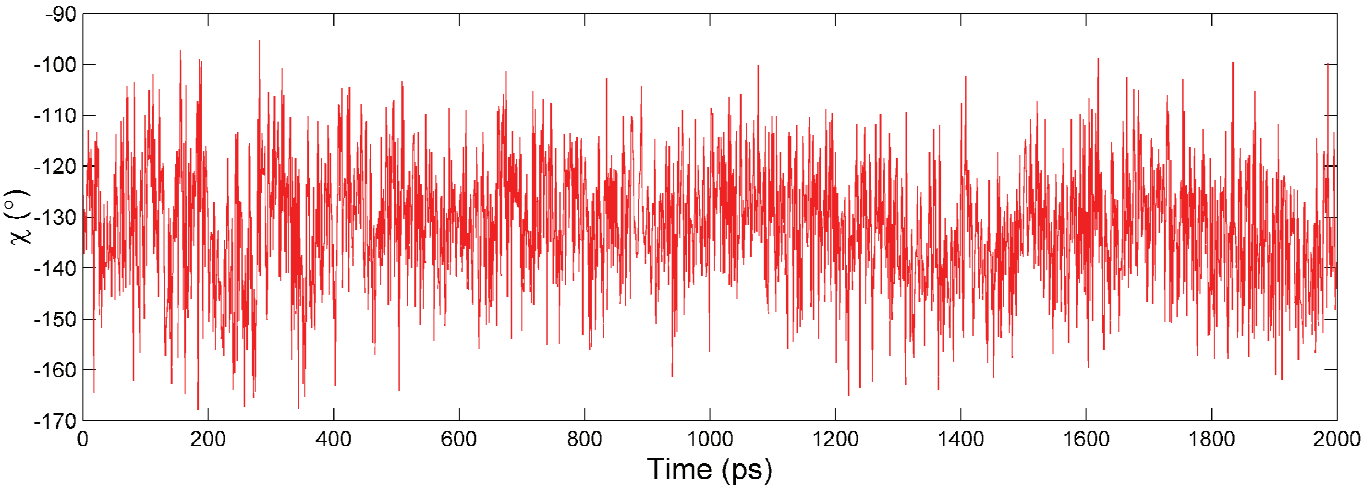

Figure S11: Time dependence of torsion angles governing the orientation of the [BP]G* adduct. Ensemble average and standard deviations are provided beside each panel. Color code: black, χ of the unmodified dG; red, χ of [BP]G*; blue, α' of [BP]G*; green, β' of [BP]G*.

Step 1: [BP]G* in the pre-insertion site of open BF

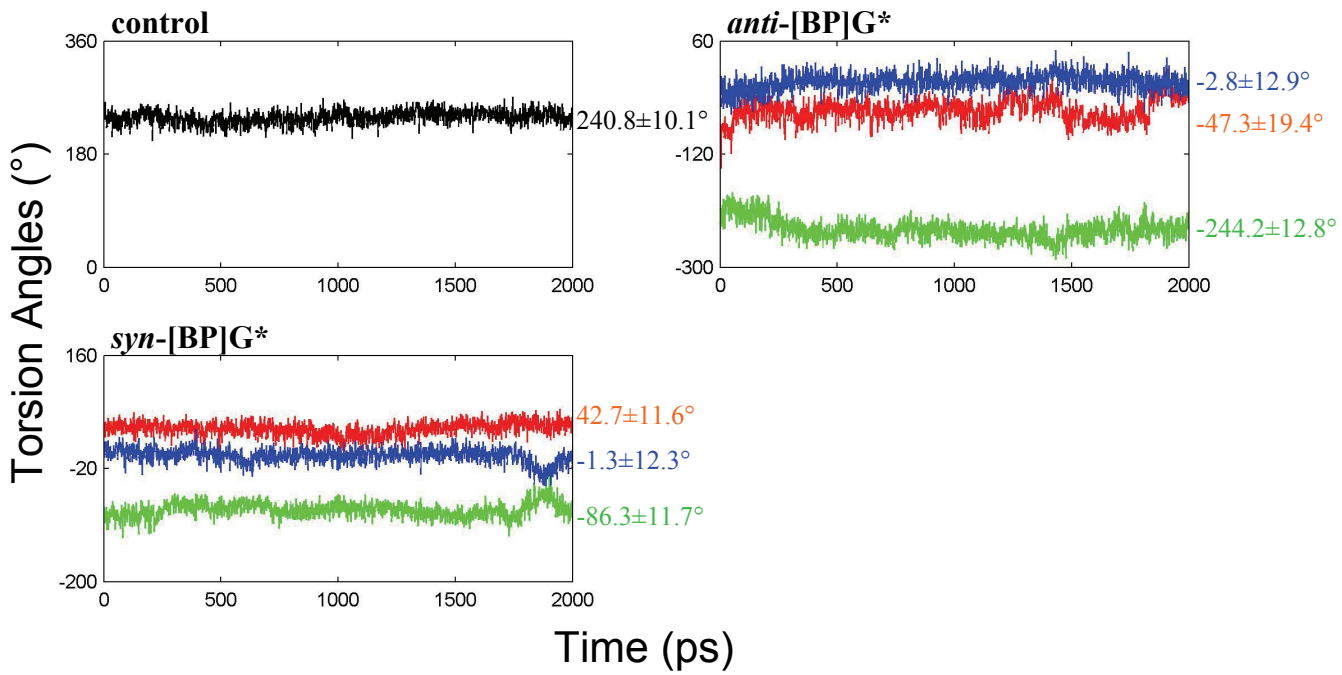

Step 2: [BP]G* in the insertion site of closed BF

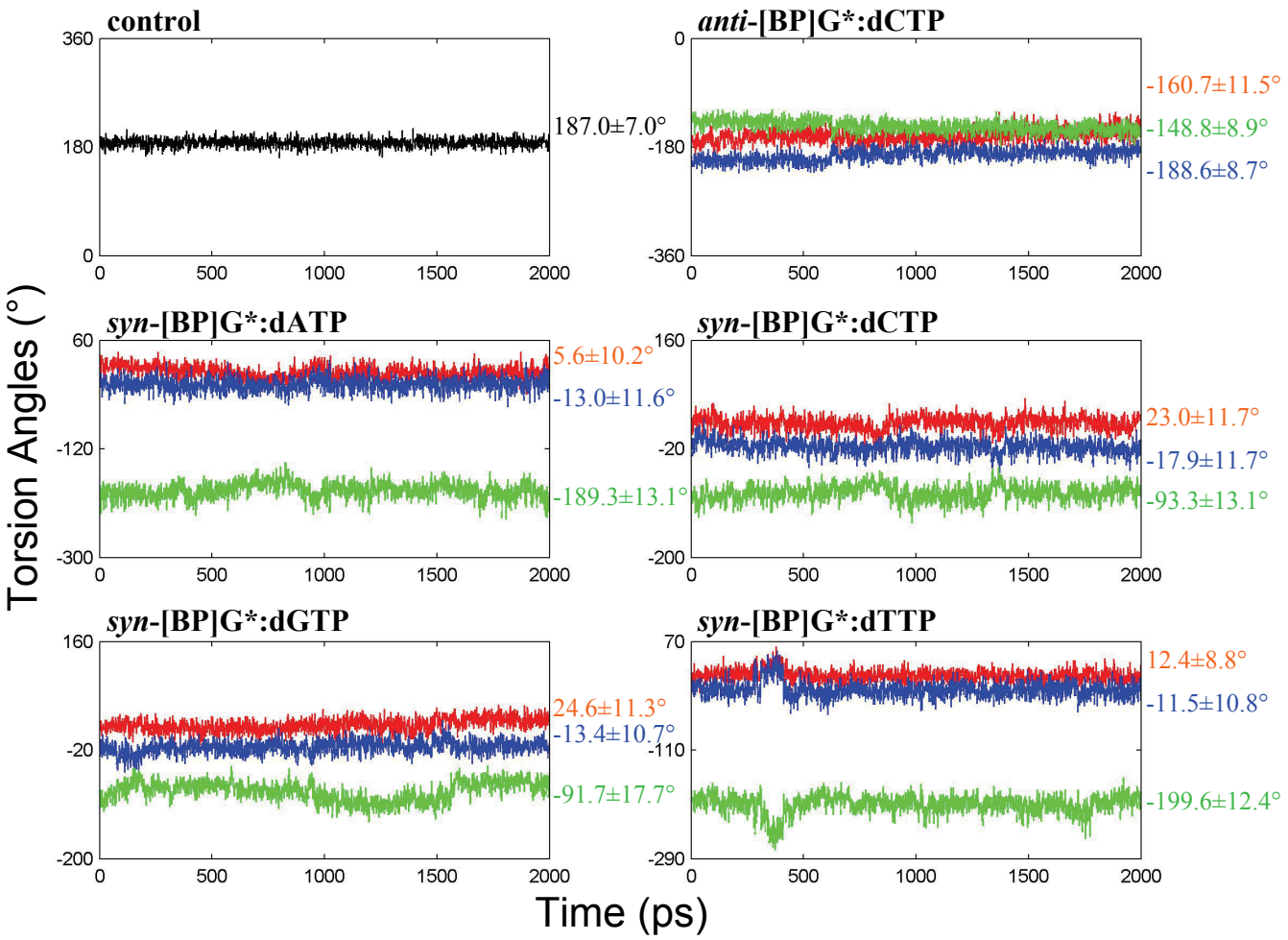

Step 3: [BP]G* in the post-insertion site of open BF

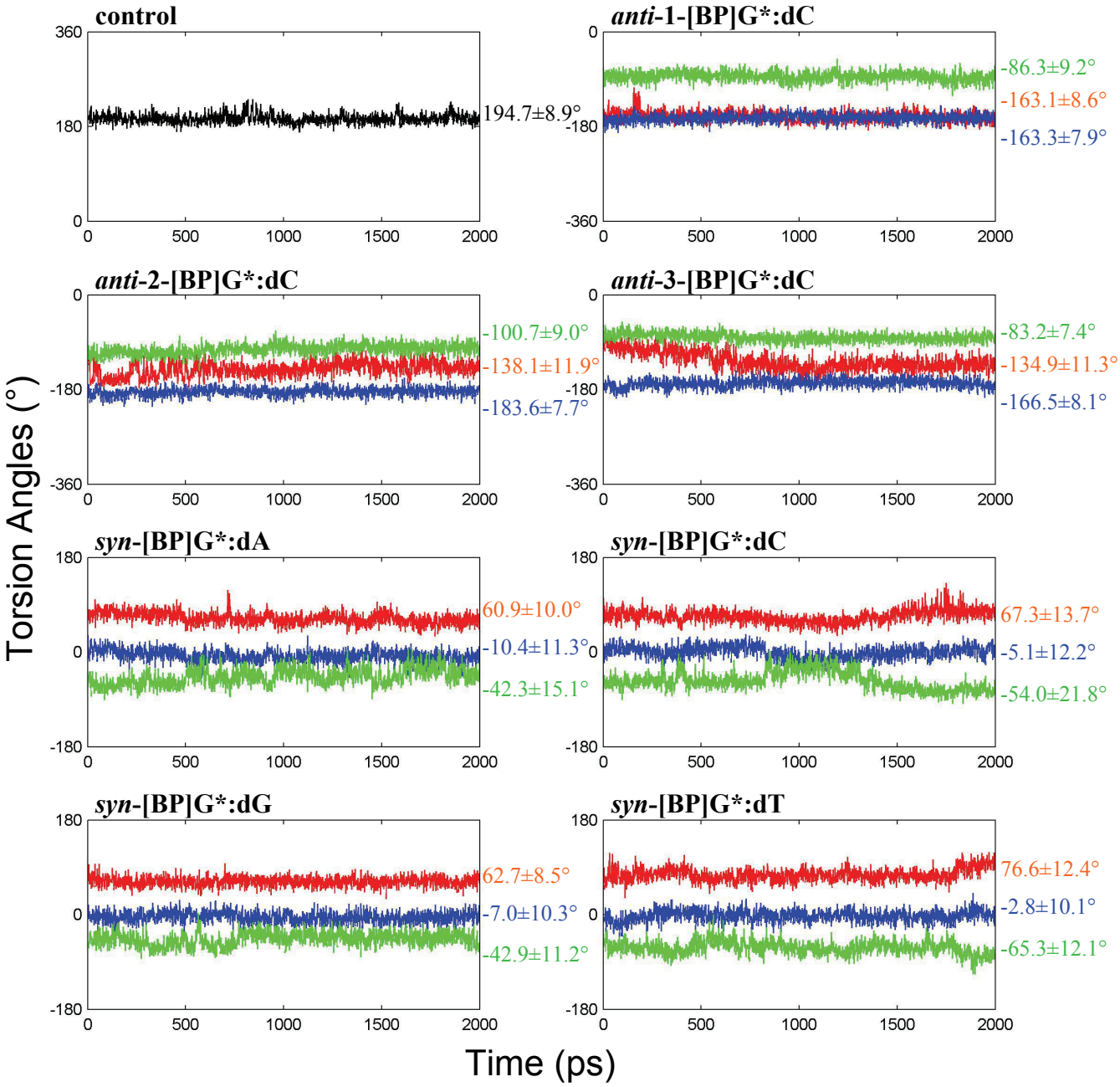

Step 4: [BP]G* in the post-insertion site of closed BF